arXiv:0903.1723v2 [hep-ph] 24 Apr 2009

The Nucleon Distribution Amplitudes and their application to nucleon form factors and the $N \to \Delta$ transition at intermediate values of Q^2

Alexander Lenz, Meinulf Göckeler, Thomas Kaltenbrunner, Nikolaus Warkentin
Fakultät für Physik, Universität Regensburg, 93040 Regensburg, Germany

We compare a recent lattice determination of the nucleon distribution amplitudes with other approaches and models. We study the nucleon distribution amplitudes up to twist 6 in next-to leading conformal spin and we also investigate conformal d-wave contributions to the leading twist distribution amplitude. With the help of light-cone sum rules one can relate the distribution amplitudes to the form factors of the nucleon or the $N \to \Delta$ transition at intermediate values of the momentum transfer. We compare our results with experimental data in the range 1 GeV$^2 \leq Q^2 \leq 10$ GeV^2. Keeping in mind that we are working only in LO QCD and NLO-QCD corrections might be sizeable we already obtain a surprisingly good agreement for the nucleon form factors G_M^n, G_M^p, G_A^p and G_T^p and for the $N \to \Delta$ transition form factor ratios R_{EM} and R_{SM}.

PACS numbers:

I. INTRODUCTION

The nucleon distribution amplitudes represent the universal non-perturbative input to numerous exclusive reactions, see, e.g., [1] for an early review. Taking corrections up to twist-6 [2] into account we compare different non-perturbative methods to determine the nucleon distribution amplitudes, in particular lattice simulations [3, 4, 5], QCD sum rule estimates [2, 6] and a phenomenological model [6]. For asymptotically large values of the momentum transfer Q^2 the form factors can be expressed as a convolution of two leading-twist distribution amplitudes with a hard - perturbatively calculable - scattering kernel [7, 8, 9, 10, 11, 12, 13, 14, 15]. This approach (pQCD) is formally proven in the $Q^2 \to \infty$ limit, and currently there is the consensus that pQCD is not valid at experimentally accessible values of the momentum transfer. In [16] light-cone sum rules [17, 18] were worked out which relate the nucleon distribution amplitudes to the experimentally accessible form factors of the nucleon at intermediate momentum transfer. Form factors are interesting quantities per se, since they encode information about the structure of the investigated baryon. This interest rised a lot in recent years, in particular because new data from JLAB [19, 20, 21, 22] for the well-known electromagnetic form factors of the nucleon contradict common textbook-wisdom. See, e.g., [23] for a review and further references. To our knowledge light-cone sum rules are the only theoretical approach to determine form factors at intermediate momentum transfer that incorporate consistently the purely perturbative approach (pQCD). This was explicitly shown in the case of the pion form factor [24]. If one calculates the light-cone sum rules for the pion form factor to leading order and next-to-leading order in QCD one can show that the α_s-corrections include the pQCD result in the $Q^2 \to \infty$ limit. In the case of baryon form factors the pQCD result is expected to be included in the $\mathcal{O}(\alpha_s^2)$ corrections to the light-cone sum rule calculation. Currently only leading-order sum rules for the baryon form factors are known and a part of the NLO QCD corrections to the nucleon form factors.

The paper is organized as follows. In section 2 we introduce the concept of distribution amplitudes, in section 3 we collect QCD sum rule predictions for the nucleon distribution amplitudes and in section 4 we shortly explain the lattice determination of the moments of the nucleon distribution amplitudes. All these approaches, including the numerical results, are discussed in section 5. The light-cone sum rule formalism is introduced in section 6 where we also give a short overview over the current literature on light-cone sum rules for baryonic form factors. In the next three sections we compare light-cone sum rule predictions with different models of the nucleon distribution amplitude for the form factors of the nucleon and for the $N \to \Delta$ transition. In section 7 we use the nucleon distribution amplitudes including next-to-leading conformal spin contributions to determine the form factors, in section 8 we make use of some relations between twist-4 and twist-3 parameters and in section 9 we investigate the effect of the d-wave contributions to the leading twist distribution amplitude. We conclude and summarize our results in section 11.

In the appendix we give for the first time the full expression for all nucleon distribution amplitudes up to twist-6 including also the d-wave contribution for the leading twist distribution amplitude.

II. THE NUCLEON DISTRIBUTION AMPLITUDES

The distribution amplitudes comprise the infrared behaviour in exclusive processes involving large momentum transfer. They remove the infrared divergences in the perturbative diagrams encoding the nonperturbative content of the process and are defined in terms of the Bethe-Salpeter wave function

$$\Psi_{\mathrm{BS}}(x,k_\perp) = \langle 0|T\left[q(x_1,k_{1,\perp})q(x_2,k_{2,\perp})q(x_3,k_{3,\perp})\right]|P\rangle \tag{1}$$

with x_i being the longitudinal momentum fraction carried by the quark i, $k_{i,\perp}$ its transverse momentum and $|P\rangle$ the nucleon state with momentum P ($P^2 = M_N^2$). The distribution amplitudes are then obtained by integrating out the transverse momenta,

$$\Phi(x_i,\mu) = Z(\mu)\int^{|k_\perp|\leq\mu} \mathrm{d}^2k_{i,\perp}\,\Psi_{\mathrm{BS}}(x,k_\perp)\,, \tag{2}$$

where Z results from the renormalisation of the quark field operators. In coordinate space the nucleon distribution amplitudes are derived from the following non-local nucleon-to-vacuum matrix element (here we follow the definitions in [2])

$$\langle 0|\epsilon_{ijk}u_\alpha^{i'}(a_1x)[a_1x,a_0x]_{i',i}u_\beta^{j'}(a_2x)[a_2x,a_0x]_{j',j}d_\gamma^{k'}(a_3x)[a_3x,a_0x]_{k',k}|P\rangle\,; \tag{3}$$

u and d are quark field operators, α, β and γ are Dirac indices, while i,j and k are color indices; x is an arbitrary light-like vector, $x^2=0$, while the a_i are real numbers that fulfill $a_1+a_2+a_3=1$. The gauge-factors $[x,y]$ are defined as

$$[x,y] = \mathcal{P}\exp\left[ig\int_0^1 dt(x-y)_\mu A^\mu(tx+(1-t)y)\right]\,, \tag{4}$$

where path ordering $\mathcal{P}$ is implied. They render the matrix element in Eq. (3) gauge invariant. In the following formulas we omit the gauge factors in order to simplify the notation.

The leading-twist contribution to the nucleon distribution amplitudes has been determined long time ago including terms of next-to-next-to leading conformal spin, see, e.g., [1] for an early review. We will compare different determinations of the arising non-perturbative parameters in section 5. Currently the nucleon distribution amplitudes have been expanded up to contributions of twist 6 in [2] and the corresponding non-perturbative parameters were estimated in [2, 6] with QCD sum rules and in [6] from a phenomenological model. Some of these parameters were also calculated on the lattice [3, 4, 5, 25, 26]. So-called x^2-corrections (corresponding to deviations from the light-like separations of the quark fields in Eq. (3)) to the leading twist distribution amplitudes were determined in [6, 16, 27, 28], they are formally of twist 5.

Using the symmetry properties of the quark fields the matrix element in (3) can be expanded in twist as

$$4\langle 0|\epsilon_{ijk}u_\alpha^i(a_1x)u_\beta^j(a_2x)d_\gamma^k(a_3x)|P\rangle = \sum_i(\Gamma_3)^i_{\alpha\beta}(\Gamma_4)^i_\gamma\;F_i\,, \tag{5}$$

where $\Gamma_{3/4}$ are certain Dirac structures and the F_i are distribution amplitudes, which can be expanded into eigenstates of conformal symmetry. This results in terms containing local operators. These local operators are associated with the moments of the distribution amplitudes, which are defined as

$$F_i^{n_1n_2n_3} = \frac{1}{F_{i,N}}\int_0^1 \mathcal{D}x\;x_1^{n_1}\;x_2^{n_2}\;x_3^{n_3}\;F_i(x_1,x_2,x_3). \tag{6}$$

Here $F_i(x_1,x_2,x_3)$ stands for a distribution amplitude and $F_{i,N}$ for its normalisation constant, which is chosen such that $F_i^{000}\equiv 1$. The integration measure is defined as

$$\mathcal{D}x = \mathrm{d}x_1\;\mathrm{d}x_2\;\mathrm{d}x_3\;\delta(1-x_1-x_2-x_3). \tag{7}$$

Thus momentum conservation implies for the moments of the distribution amplitudes the relation

$$F_i^{n_1n_2n_3} = F_i^{(n_1+1)n_2n_3} + F_i^{n_1(n_2+1)n_3} + F_i^{n_1n_2(n_3+1)}. \tag{8}$$

Further details on distributions amplitudes (with complete expressions and definitions up to twist 6) are summarized in the appendices.

For the nucleon distribution amplitudes isospin symmetry and the presence of two quarks of the same type implies that the number of independent distribution amplitudes is reduced compared to the general case. In particular, the leading-twist nucleon distribution amplitudes can be expressed in terms of only one independent distribution amplitude which is usually taken as

$$\varphi(x_1,x_2,x_3) = V_1(x_1,x_2,x_3) - A_1(x_1,x_2,x_3) \tag{9}$$

and is equal to $\Phi_3(x_1,x_2,x_3)$ in the notation of [2]. The distribution amplitudes A_1 and V_1 are defined in the appendices. At leading twist the nucleon distribution amplitude $\varphi(x_i)$ corresponds to the following form of the proton state [29, 30]:

$$|\,P,\uparrow\,\rangle = \int_0^1 \mathcal{D}x \frac{\varphi(x_i)}{\sqrt{96 x_1 x_2 x_3}} |u^\uparrow(x_1)\left[u^\downarrow(x_2) d^\uparrow(x_3) - d^\downarrow(x_2) u^\uparrow(x_3)\right]\rangle\,. \tag{10}$$

The first moments of $\varphi(x_i)$ can be interpreted as the momentum fractions carried by the quarks.
The leading-twist distribution amplitude depends at leading conformal spin on one non-perturbative parameter, the normalization constant f_N, while for twist four we have two additional constants λ_1 and λ_2. In our approach no new parameters appear in leading conformal spin up to twist six. At next-to-leading conformal spin only two non-perturbative parameters $V_1^d = \varphi^{001}$ and $A_1^u = \varphi^{100} - \varphi^{010}$ arise in the case of leading twist and at next-to-leading twist we have three non-perturbative parameters, f_1^d, f_1^u and f_2^d, for details see [2, 6]. For the leading-twist distribution amplitude $\varphi(x_i)$ we have also determined the next-to-next-to leading conformal spin contributions which can be completely parametrized, e.g., by the moments φ^{101}, φ^{200} and φ^{002}. The local matrix elements defining the non-perturbative parameters up to next-to leading conformal spin are (see [6] for the corrected formulas from [2])

$$\langle 0|\varepsilon^{ijk}\left[u^i C\not{z}\, u^j\right](0)\,[\gamma_5\not{z} d^k]_\delta(0)|P\rangle = f_N (P\cdot z)\not{z} N_\delta(P)\,, \tag{11}$$
$$\langle 0|\varepsilon^{ijk}\left[u^i C\gamma_\mu\, u^j\right](0)\,[\gamma_5\gamma^\mu d^k]_\delta(0)|P\rangle = \lambda_1 m_N N_\delta(P)\,, \tag{12}$$
$$\langle 0|\varepsilon^{ijk}\left[u^i C\sigma_{\mu\nu}\, u^j\right](0)\,[\gamma_5\sigma^{\mu\nu} d^k]_\delta(0)|P\rangle = \lambda_2 m_N N_\delta(P)\,, \tag{13}$$
$$\langle 0|\varepsilon^{ijk}\left[u^i C\not{z}\, u^j\right](0)\,[\gamma_5\not{z} iz\cdot\vec{D} d^k]_\delta(0)|P\rangle = f_N V_1^d (P\cdot z)^2\not{z} N_\delta(P)\,, \tag{14}$$
$$\langle 0|\varepsilon^{ijk}\left[u^i C\not{z}\,\gamma_5 iz\cdot\overset{\leftrightarrow}{D}\, u^j\right](0)\,[\not{z} d^k]_\delta(0)|P\rangle = -f_N A_1^u (P\cdot z)^2\not{z} N_\delta(P)\,, \tag{15}$$
$$\langle 0|\,\varepsilon^{ijk}\left[u^i C\gamma_\mu u^j\right](0)[\not{z}\gamma_5\gamma^\mu iz\cdot\vec{D} d^k]_\delta(0)\,|P\rangle = \lambda_1 f_1^d (P\cdot z) M\,\not{z} N_\delta(P)\,, \tag{16}$$
$$\langle 0|\,\varepsilon^{ijk}\left[u^i C\sigma_{\mu\nu} u^j\right](0)[\not{z}\gamma_5\sigma^{\mu\nu} iz\cdot\vec{D} d^k]_\delta(0)\,|P\rangle = \lambda_2 f_2^d (P\cdot z) M\not{z} N_\delta(P)\,, \tag{17}$$
$$\langle 0|\,\varepsilon^{ijk}\left[u^i C\gamma_\mu\gamma_5 iz\cdot\overset{\leftrightarrow}{D}\, u^j\right](0)[\not{z}\gamma^\mu d^k]_\delta(0)\,|P\rangle = \lambda_1 f_1^u (P\cdot z) M\,\not{z} N_\delta(P)\,, \tag{18}$$

with the nucleon spinor $N_\delta(P)$, the nucleon mass m_N, an arbitrary light-like vector z^ν with $z^2 = 0$ and $\overset{\leftrightarrow}{D} = \vec{D} - \overset{\leftarrow}{D}$. All derivatives act only on the quark fields and not on any explicit factor z. The second moments of the nucleon distribution amplitudes are related to the following local operators:

$$\langle 0|\varepsilon^{ijk}\left[u^i C\not{z}\, u^j\right](0)\,[\gamma_5\not{z}\,(iz\cdot\vec{D})^2 d^k]_\delta(0)|P\rangle = f_N\varphi^{002}(P\cdot z)^3\not{z} N_\delta(P)\,, \tag{19}$$
$$\begin{aligned}&\langle 0|\varepsilon^{ijk}\left[((iz\cdot\vec{D})^2 u^i) C\not{z}\, u^j\right](0)\,[\gamma_5\not{z} d^k]_\delta(0)|P\rangle \\ &-\langle 0|\varepsilon^{ijk}\left[((iz\cdot\vec{D})^2 u^i) C\not{z}\gamma_5 u^j\right](0)\,[\not{z} d^k]_\delta(0)|P\rangle = f_N\varphi^{200}(P\cdot z)^3\not{z} N_\delta(P)\,,\end{aligned} \tag{20}$$
$$\begin{aligned}&\langle 0|\varepsilon^{ijk}\left[(iz\cdot\vec{D} u^i) C\not{z} u^j\right](0)\,[\gamma_5\not{z} iz\cdot\vec{D} d^k]_\delta(0)|P\rangle \\ &-\langle 0|\varepsilon^{ijk}\left[(iz\cdot\vec{D} u^i) C\not{z}\gamma_5 u^j\right](0)\,[\not{z}\; iz\cdot\vec{D} d^k]_\delta(0)|P\rangle = f_N\varphi^{101}(P\cdot z)^3\not{z} N_\delta(P)\,.\end{aligned} \tag{21}$$

The parameters used in this work with their twist and conformal spin are summarised in the table below

	Leading twist	Higher twist
Leading conformal spin	f_N	λ_1, λ_2
Next-to-leading conformal spin	A_1^u, V_1^d	f_1^u, f_1^d, f_2^d
Next-to-next-to-leading conformal spin	φ^{101}, φ^{200}, φ^{002}	–

As in the meson case these parameters can be estimated with QCD sum rules [31] (see, e.g., [32, 33, 34] for some recent work in the meson case) or with lattice simulations (see, e.g., [35, 36] for lattice works considering the same mesons).

III. QCD SUM RULE DETERMINATION OF THE NUCLEON DISTRIBUTION AMPLITUDES

The leading-twist distribution amplitude was investigated with QCD sum rules up to the second moments in [29, 37] and up to the third moments in [30] including perturbative contributions and terms proportional to the gluon condensate and to the four-quark condensate (several errors in [29] were corrected in [30]).
The next-to-leading twist normalization constants λ_1 and λ_2 describe the coupling to the proton of two independent proton interpolating fields used in QCD sum rules, λ_1 is the coupling of the so-called Ioffe current [38], while λ_2 is the coupling of the interpolating nucleon field that was advocated in [39]. In [38] and [39] first QCD sum rule estimates for $\lambda_{1,2}$ were presented. Higher dimensional condensates were included in [40]. Unfortunately these pioneering works contain several misprints, for a review with the correct expressions see, e.g., [41, 42]. α_s-corrections were calculated by Jamin in [43]. They turned out to be very large ($\approx +50\%$ for $|\lambda_1^2|$, corresponding to $\approx +25\%$ for $|\lambda_1|$), but we will not take them into account, since we also do not have α_s-corrections for the light-cone sum rules, connecting the distribution amplitudes with the nucleon form factors. In [6] also contributions of non-planar diagrams to the dimension 8 condensates were included. Putting all this together (for the first time) the QCD sum rule expression for λ_1 reads

$$\begin{aligned} 2(2\pi)^4 m_N^2 |\lambda_1^2| = \; & e^{\frac{m_N^2}{M_B^2}} \; \left\{ M_B^6 E_3\left(\frac{s_0}{M_B^2}\right) L^{-\frac{4}{9}} \left(1+\left[\frac{53}{12}+\gamma_E\right]\frac{\alpha_s(M_B^2)}{\pi}\right)\right. \\ & + \left. \frac{b}{4} M_B^2 E_1\left(\frac{s_0}{M_B^2}\right) L^{-\frac{4}{9}} + \frac{a^2}{3}\left[4-\frac{4}{3}\frac{m_0^2}{M_B^2}\right]\right\} , \qquad (22) \end{aligned}$$

where M_B is the Borel parameter, s_0 is the continuum threshold and

$$E_n(s_0/M^2) \;=\; 1-e^{(-s_0/M^2)}\sum_{k=0}^{n-1}\frac{1}{k!}\left(\frac{s_0}{M^2}\right)^k , \qquad (23)$$

$$L \;=\; \frac{\alpha_s(\mu^2)}{\alpha_s(M_B^2)} , \qquad (24)$$

$$a \;=\; -(2\pi)^2\langle\bar{q}q\rangle \simeq 0.55 \text{ GeV}^3 , \qquad (25)$$

$$b \;=\; (2\pi)^2\langle\frac{\alpha_S}{\pi}G^2\rangle \simeq 0.47 \text{ GeV}^4 , \qquad (26)$$

$$m_0^2 \;=\; \frac{\langle\bar{q}gGq\rangle}{\langle\bar{q}q\rangle} \simeq 0.65 \text{ GeV}^2 . \qquad (27)$$

We have neglected in Eq. (22) the small α_s-corrections to the four-quark contribution proportional to a^2. The corresponding formula for λ_2 can be found, e.g., in [6]. QCD sum rule estimates for the f_x^y defined in Eqs. (16) - (18) were first presented in [2] and updated in [6]. The parameter set which is obtained by QCD sum rules will be called *sum-rule* estimate in the following, we use the numerical values from [30] for the moments of the leading-twist distribution amplitude and the values from [6] for f_N, λ_1, λ_2, A_1^u, V_1^d, f_1^d, f_1^u and f_2^d.
In our analysis we use two related parameter sets which are based on the QCD sum rule determination:

- Demanding that all higher conformal contributions vanish, fixes A_1^u, V_1^d, f_1^d, f_1^u and f_2^d, while the values for f_N, λ_1, λ_2 are taken from the QCD sum rule estimates or from the lattice calculation. This parameter set will be called *asymptotic*. In the case of the leading twist, one would be left with the asymptotic distribution amplitude $\varphi(x_i, Q^2 \to \infty) = \varphi_{asy}(x_i) = 120 x_1 x_2 x_3 f_N$. The corresponding expressions for the higher twist distribution amplitudes can be found in [2].
- With the help of light-cone sum rules [6, 16, 44] one can express the nucleon form factors in terms of the eight non-perturbative parameters f_N, λ_1, λ_2, A_1^u, V_1^d, f_1^d, f_1^u and f_2^d (inlcuding twist-6 corrections and expanding the distribution amplitudes up to the next-to-leading conformal spin). Choosing values for these parameters in between the *asymptotic* and the *sum-rule* values, we got an astonishingly good agreement with the experimental numbers, see [6]. This procedure is obviously rather ad-hoc and has to be replaced by a real fit after α_s-corrections to the light-cone sum rules have been calculated. The paramter set obtained in [6] will be called *BLW*.

IV. LATTICE DETERMINATION OF THE NUCLEON DISTRIBUTION AMPLITUDES

Lattice QCD offers the possibility to perform non-perturbative computations in QCD without additional model assumptions. For example, one can evaluate hadron masses and matrix elements of local operators between hadron states. In particular, the non-perturbative parameters $f_N, \ldots$ introduced above can be extracted from Monte Carlo simulations on the lattice as advocated in [45].

Recently, the QCDSF collaboration has performed such a calculation [4]. It is based on gauge field configurations generated with two dynamical flavours of quarks. For the gauge field the standard Wilson action was used, while the lattice action for the quarks was the so-called non-perturbatively $O(a)$ improved Wilson fermion action, also known as the clover fermion action. Although lattice artefacts seem to be small, a reliable continuum extrapolation could not be attempted, and we utilize here the data obtained on the finest lattice corresponding to a gauge coupling parameter $\beta = 5.40$. Setting the scale via a Sommer parameter of $r_0 = 0.467\,\mathrm{fm}$ the lattice spacing turns out to be $a \approx 0.067\,\mathrm{fm}$. On the lattice, matrix elements between the vacuum and a nucleon such as those needed here are computed from two-point correlation functions of the local operator $\mathcal{O}_\alpha(x)$ under study and a suitable interpolating field $\bar{\mathcal{N}}_\alpha(x)$ for the nucleon. Asymptotically this two-point function decays exponentially with the distance between the operators since the lattice calculations are performed in Euclidean space. Projecting onto definite momentum one finds for sufficiently large (Euclidean) times t:

$$\sum_{\vec{x}}\sum_{\vec{y}} e^{-i\vec{P}\cdot\vec{x}} e^{i\vec{P}\cdot\vec{y}} \langle \mathrm{O}_\alpha(\vec{x},t)\bar{\mathcal{N}}_\beta(\vec{y},0)\rangle = \frac{V_s\sqrt{Z}}{2E(\vec{P})} M_{\mathcal{O}} \left(E(\vec{P})\gamma_4 - i\vec{P}\cdot\vec{\gamma} + m_N \right)_{\alpha\beta} e^{-E(\vec{P})t}\,. \tag{28}$$

Here V_s denotes the spatial volume of the lattice and the matrix elements of $\mathcal{O}_\alpha(x)$ and $\bar{\mathcal{N}}_\alpha(x)$ have been represented as

$$\langle 0|\mathcal{O}_\alpha(0)|P\rangle = M_{\mathcal{O}} N_\alpha(P)\,, \tag{29}$$

$$\langle P|\bar{\mathcal{N}}_\alpha(0)|0\rangle = \sqrt{Z}\bar{N}_\alpha(P). \tag{30}$$

As the local operators $\mathcal{O}_\alpha(x)$ used in the simulations are linear combinations of the operators appearing in (11)-(21), the constants $M_{\mathcal{O}}$ are directly related to moments of the distribution amplitudes.

The operators $\mathcal{O}_\alpha(x)$ need to be renormalized. In Ref. [4] a non-perturbative renormalization procedure has been chosen. As the space-time symmetry on the lattice is reduced to the finite (spinorial) hypercubic group, the mixing pattern of our three-quark operators is more complicated than in the continuum and the choice of the operators becomes an important issue. Guided by the group-theoretical classification of three-quark operators given in [46] the problematic mixing with lower-dimensional operators could however be completely avoided. Moreover, the freedom in the choice of the operators has ben exploited in order to reduce the statistical uncertainties of the results.

Primarily, the combination of moments

$$\phi^{n_1n_2n_3} = \frac{1}{3}\left(V_1^{n_1n_2n_3} - A_1^{n_1n_2n_3} + 2\,T_1^{n_1n_3n_2}\right) = \frac{1}{3}\left(2\,\varphi^{n_1n_2n_3} + \varphi^{n_3n_2n_1}\right) \tag{31}$$

has been evaluated, from which the combination $\varphi^{n_1n_2n_3}$ usually used in sum rule calculations is readily obtained by

$$\varphi^{n_1n_2n_3} = 2\phi^{n_1n_2n_3} - \phi^{n_3n_2n_1}. \tag{32}$$

In the following sections we shall compare these lattice results with results obtained from other approaches and see what the lattice numbers imply for the nucleon form factors.

V. COMPARISON OF DIFFERENT METHODS TO DETERMINE THE DISTRIBUTION AMPLITUDES

In Table I we compare different estimates for the moments of the leading-twist distribution amplitude at 1 GeV^2. It turns out that the BLW model, the BK model and the lattice evaluation give almost indentical results, which are close to the asymptotic values, while the QCD sum rule estimates seem to overestimate the deviation from the asymptotic form, although the deviation goes in the right direction. The BLW model was inspired by this experience: One starts with the asymptotic form and goes then in the direction of the QCD sum rule estimate, but only for a fraction of the whole difference. Choosing this fraction to be 1/3 one gets an astonishingly good agreement between light-cone sum rule predictions for the nucleon form factors and experiment, see [6]. In the same spirit one can make a BLW model for the second moments, also given in table I [117] . These values are again very close to the lattice values. The BK model [47] was also inspired by experiment, in particular the decay $J/\Psi \to N\bar{N}$, the Feynman contribution to the nucleon form factor and the valence quark distribution function. In Table II we compare different estimates for f_N,

	Asy	QCD-SR	COZ	KS	BK	BLW	LAT
φ^{100}	$\frac{1}{3} \approx 0.333$	0.560(60)	0.579	0.55	$\frac{8}{21} \approx 0.38$	0.415	0.3999(37)(139)
φ^{010}	$\frac{1}{3} \approx 0.333$	0.192(12)	0.192	0.21	$\frac{13}{42} \approx 0.31$	0.285	0.2986(11)(52)
φ^{001}	$\frac{1}{3} \approx 0.333$	0.229(29)	0.229	0.24	$\frac{13}{42} \approx 0.31$	0.300	0.3015(32)(106)
φ^{200}	$\frac{1}{7} \approx 0.143$	0.350(70)	0.369	0.35	$\frac{5}{28} \approx 0.18^\star$	0.225	0.1816(64)(212)
φ^{020}	$\frac{1}{7} \approx 0.143$	0.084(19)	0.068	0.09	$\frac{1}{8} \approx 0.13^\star$	0.121	0.1281(32)(106)
φ^{002}	$\frac{1}{7} \approx 0.143$	0.109(19)	0.089	0.12	$\frac{1}{8} \approx 0.13^\star$	0.132	0.1311(113)(382)
φ^{011}	$\frac{2}{21} \approx 0.095$	−0.030(30)	0.027	0.02	$\frac{1}{12} \approx 0.08^\star$	0.071	0.0613(89)(319)
φ^{101}	$\frac{2}{21} \approx 0.095$	0.102(12)	0.113	0.10	$\frac{17}{168} \approx 0.10^\star$	0.097	0.1091(41)(152)
φ^{110}	$\frac{2}{21} \approx 0.095$	0.090(10)	0.097	0.10	$\frac{8}{21} \approx 0.10^\star$	0.093	0.1092(67)(219)

TABLE I: Comparison of different estimates for the moments of the leading-twist distribution amplitude renormalized at 1 GeV^2. We show the asymptotic values (Asy) and the QCD sum rule estimates from [30]. Inspired by the QCD sum rule calculation two models for the leading-twist distribution amplitude were suggested, the COZ model [30] and the KS model [37]. Using also some experimental input two phenomenological models were introduced, the BK model [47] and the BLW model [6]. Finally we show the lattice values from [3, 4, 5]. The first error is statistical, the second error represents the uncertainty due to the chiral extrapolation and renormalization. For the BK model no contributions from next-to-next-to-leading conformal spin were taken into account, thus the second moments denoted by the * do not contain any additional information and are fully determined by the first moments.

	As.	QCD-SR	BK	BLW	LAT
$f_N \cdot 10^3[\mathrm{GeV}^2]$	5.0(5)	5.0(5)	6.64	5.0(5)	3.234(63)(86)
$\lambda_1 \cdot 10^3[\mathrm{GeV}^2]$	−27(9)	−27(9)	–	−27(9)	−35.57(65)(136)
$\lambda_2 \cdot 10^3[\mathrm{GeV}^2]$	54(19)	54(19)	–	54(19)	70.02(128)(268)
A_1^u	0	0.38(15)	$\frac{1}{14} \approx 0.071$	0.13	0.1013(81)(298)
V_1^d	$\frac{1}{3} \approx 0.333$	0.23(3)	$\frac{13}{42} \approx 0.31$	0.30	0.3015(32)(106)
f_1^d	0.30	0.40(5)	–	0.33	–
f_1^u	0.10	0.07(5)	–	0.09	–
f_2^d	$\frac{4}{15} \approx 0.267$	0.22(5)	–	0.25	–

TABLE II: Comparison of different estimates for f_N, λ_1, λ_2, A_1^u, V_1^d, f_1^d, f_1^u and f_2^d renormalized at 1 GeV^2. The QCD sum rule estimates and the BLW values are taken from [6] and we also show the phenomenological model from [47] (BK). For the asympotic and the BLW parameters the values for f_N, λ_1 and λ_2 coincide with the ones from the QCD sum rule estimates.

λ_1, λ_2, A_1^u, V_1^d, f_1^d, f_1^u and f_2^d at 1 GeV^2. The leading twist parameters A_1^u, V_1^d, are already fully contained in table I via the relations

$$A_1^u = 2\varphi^{100} + \varphi^{001} - 1\,, \tag{33}$$

$$V_1^d = \varphi^{001}\,. \tag{34}$$

Let us stress, however, that the errors quoted in Tables I and II have to be taken with caution. On the lattice side a continuum extrapolation could not be attempted, and hence the associated systematic error is not included. Moreover, the errors on A_1^u have been calculated by error propagation, which might not be too reliable. For the sum rule estimates the radiative corrections are expected to be sizeable, but these are only known for λ_1 and λ_2. The central lattice value of f_N is about 35% smaller than the QCD sum rule estimates, while the lattice results for $|\lambda_1|$ and $|\lambda_2|$ are about 30% larger than the QCD sum rule estimates. For λ_1 and λ_2 the discrepancy is reduced strongly, if radiative corrections to the sum rule estimates are included, cf. Eq. (22), for f_N - according to our knowledge - no radiative corrections have been calculated yet.

The parameters λ_1 and λ_2 can also be extracted from the lattice calculation of the nucleon decay matrix elements (expressed in terms of the parameters α and β) in [25, 26]. Using the relations

$$\lambda_1 = \frac{4}{m_N}\alpha\,, \qquad \lambda_2 = \frac{8}{m_N}\beta\,, \tag{35}$$

we obtain from the results in [25, 26]

$$\lambda_1 = -43.90 \pm 4.7 \pm 8.5 \cdot 10^{-3}\mathrm{GeV}^2\,, \qquad \lambda_2 = 93.96 \pm 10.2 \pm 22.7 \cdot 10^{-3}\mathrm{GeV}^2\,,$$

at the renormalization scale 1 GeV^2. In that case the deviation from the QCD sum rule values is even more pronounced. In the non-relativistic limit one gets

$$2\lambda_1 + \lambda_2 = 0\,.$$

The estimates presented in table II fulfill this relation almost perfectly:

$$\left|\frac{2\lambda_1+\lambda_2}{2\lambda_1-\lambda_2}\right|_{\text{QCD-SR}} = 0 \pm 0.24\,, \tag{36}$$

$$\left|\frac{2\lambda_1+\lambda_2}{2\lambda_1-\lambda_2}\right|_{\text{LAT}} = 0.008 \pm 0.013\,. \tag{37}$$

For the ratio f_N/λ_1 the differences between the central lattice and QCD sum rule estimates are even more enhanced:

$$\left(\frac{f_N}{\lambda_1}\right)_{\text{QCD-SR}} = -0.185 \pm 0.064\,, \tag{38}$$

$$\left(\frac{f_N}{\lambda_1}\right)_{\text{LAT}} = -0.0909 \pm 0.0054 \pm 0.0095\,. \tag{39}$$

The QCD sum rule estimate is a factor of two larger than the lattice result. In the next section we will see that the electromagnetic form factors of the nucleon depend only on the ratio but not on the individual values of f_N and λ_1, if the so-called Ioffe interpolating field is used, while the $N \to \Delta$ transition depends on the individual values.

VI. LIGHT-CONE SUM RULES FOR FORM FACTORS

Light-cone sum rules (LCSR) are an advancement of QCD sum rules [31] for intermediate values of the momentum transfer Q^2, i.e., 1 GeV$^2 < Q^2 <$ 10 GeV^2 in the case of nucleon form factors. They were introduced in [17, 18]. The starting point is a correlation function of the form

$$T(P,q) = \int d^4x e^{-iqx} \langle 0|T\{\eta(0)j(x)\}|N(P)\rangle\,, \tag{40}$$

which describes the transition of a baryon B with momentum $P-q$ to the nucleon $N(P)$ via the current j. The baryon B is created by the interpolating three-quark field η. If B is a nucleon one can use, e.g., the Ioffe current [38] for the proton

$$\eta_{\text{Ioffe}}(x) = \epsilon^{ijk}\left[u^i(x)(C\gamma_\nu)\,u^j(x)\right]\,(\gamma_5\gamma^\nu)\,d^k_\delta(x)\,. \tag{41}$$

A typical example for j is the electromagnetic current in the case of the electromagnetic form factors

$$j^{\text{em}}_\mu(x) = e_u\bar{u}(x)\gamma_\mu u(x) + e_d\bar{d}(x)\gamma_\mu d(x)\,. \tag{42}$$

With the definitions in Eqs. (41), (42) the correlation function in Eq. (40) describes the electromagnetic form factors of the nucleon, which can be measured, e.g., in elastic electron-proton scattering.

The basic idea of the light-cone sum rule approach is to calculate the correlation function in Eq. (40) both on the hadron level (expressed in terms of form factors) and on the quark level (expressed in terms of the nucleon distribution amplitudes). Equating both results and performing a Borel transformation to suppress higher mass states one can express the form factors in terms of the eight (taking only leading and next-to leading conformal spin into account) non-perturbative parameters of the nucleon distribution amplitudes, the Borel parameter M_B and the continuum threshold s_0, for details see [6, 16].

We studied the electromagnetic nucleon form factors with the Chernyak-Zhitnitsky interpolating field (η_{CZ}) in [16]. In [44] we found that η_{CZ} yields large unphysical isospin violating effects, therefore we introduced a new isospin respecting CZ-like current to determine the electromagnetic form factors. In [6] we also studied the Ioffe current for the nucleon and extended our studies from the electromagnetic form factors to axial form factors, pseudoscalar form factors and the neutron to proton transition. It turned out that the Ioffe current yields the most reliable results. Despite our "bad experience" η_{CZ} was used to determine the scalar form factor of the nucleon [48] and the axial and the pseudoscalar one in [49]. The question of the ideal interpolating field can also be addressed more generally: One can write down the most general interpolating field - without derivatives - of the nucleon as a linear combination of two currents and then try to optimize the relative strength of these currents. This approach was used for the scalar form factor of the nucleon in [50], for the axial-vector form factors in [51] and for the electromagnetic form factors in [52]. Since in [52] x^2-corrections were not included and different Dirac projections to extract the sum rules were used, we cannot easily compare the result with [6].

The light-cone sum rule method can also be applied to other observables than the nucleon form factors.

In the class of nucleon to resonance transitions the following processes were considered: The $N \to \Delta$ transition was studied in this framework in [53] (for a similar approach for $Q^2 = 0$ see, e.g., [54]), the axial part of the $N \to \Delta$ transition was calculated in [55]. Very recently the form factors of the $N \to N^*(1535)$ transition were presented in [56]. In [57, 58, 59] pion-electroproduction was investigated.

Also decays of baryons can be described with that formalism: $\Lambda_b \to pl\nu$ was discussed in [27]. The authors of [60] considered $\Lambda_c \to \Lambda l\nu$ and therefore determined a part of the Λ distribution amplitude. In [61] the transition $\Sigma \to N$ was investigated. Recently the rare decays $\Lambda_b \to \Lambda\gamma$ and $\Lambda_b \to \Lambda l^+ l^-$ were treated in [62] with the same formalism. Electromagnetic form factors of Σ and Λ-baryons were estimated in [63, 64].

So far all mentioned LCSR calculations for the baryon form factors were done in leading order QCD. One expects sizeable radiative corrections of up to 30 %. In [65] a first step in calculating the full $\mathcal{O}(\alpha_s)$-corrections to the nucleon electromagnetic form factors was performed. The intrinsic final uncertainty of this approach is expected to be in the range of less than ±20%, if QCD corrections are included. Comparing the theoretical predictions with experimental numbers one must be careful to distinguish between quantities directly calculated like F_1 and F_2 and quantities like $G_E = F_1 - Q^2/(4m_N^2)F_2$ for which cancellations might ruin the predictive power.

In the following we use the LO QCD light-cone sum rules of [6] for the electromagnetic form factors of the nucleon and the LO QCD results of [53] for the $N \to \Delta$ transition to compare the consequences for the form factors which the lattice results for the nucleon distribution amplitudes entail with those which result from different QCD sum rule estimates. Note, however, that the errors on the non-perturbative parameters of the nucleon distribution amplitudes will not be taken into account, because this would not make much sense due to the inherent uncertainty in the LO light-cone sum rules.

VII. RESULTS FOR THE FORM FACTORS AT INTERMEDIATE MOMENTUM TRANSFER

In this section we use light-cone sum rules to extract physical form factors from the nucleon distribution amplitudes, by taking into account conformal spin contributions up to the p-wave; d-wave effects will be discussed in section 9. We compare our theory results to the following experimental numbers. For the electromagnetic nucleon form factors we take data from:

- The magnetic form factor of the proton normalized to the dipole form factor $G_M^p/(\mu_p G_D)$ from [66, 67, 68, 69, 70, 71, 72, 73, 74], with

$$G_D(Q^2) = \frac{1}{\left(1 + \frac{Q^2}{0.71\text{GeV}^2}\right)^2}\,, \qquad \mu_p = 2.7928... \tag{43}$$

  The data of [68, 69, 70] are actually taken from the reanalysis in [75].

- The ratio of the electric and magnetic form factors of the proton $\mu_p G_E^p/G_M^p$ from Rosenbluth separation [66, 67, 68, 69, 70, 71, 72, 73, 74, 76, 77, 78] and from polarization transfer [19, 20, 21, 22]. We would like to point out here that [73, 74] claimed already in the seventies a steeper Q^2 dependence of G_E^p compared to G_M^p for momentum transfers above 1 GeV^2. Currently the Rosenbluth separation data for G_E are judged to be less reliable.

- The ratio of the proton form factors F_1^p and F_2^p given as $\sqrt{Q^2}F_1^p/((\mu_p - 1)F_2^p)$ in [66, 67, 79].

- The magnetic form factor of the neutron normalized to the dipole form factor: $G_M^n/(\mu_n G_D)$ from [73, 80, 81, 82, 83, 84, 85, 86] with $\mu_n = -1.913...$

- The electric form factor of the neutron normalized to the dipole form factor: G_E^n/G_D from [73, 80, 83, 87, 88, 89, 90, 91, 92, 93, 94, 95, 96, 97, 98, 99, 100]. The data are very well described by the so-called Galster fit [101], we show in our plots the update of the Galster-fit from Kelly [102]:

$$G_E^{n,Galster}(Q^2) = \frac{(1.70 \pm 0.04)\,\tau}{1 + (3.30 \pm 0.32)\,\tau} G_D(Q^2)\,, \qquad \text{with } \tau = \frac{Q^2}{4m_p^2}\,. \tag{44}$$

For the axial form factors we compare our result to the dipole formula [103]

$$G_A(Q^2) = \frac{1.267}{\left(1 + \frac{Q^2}{(1.014GeV)^2}\right)^2}\,. \tag{45}$$

For more details see [6].
Finally we use the following data for the $N \to \Delta$ transition:

- The magnetic form factor normalized to the dipole form factor $G_M^*/(3G_D)$ from [104, 105, 106, 107, 108, 109, 110, 111].
- The ratio of the electric quadrupole to the magnetic form factor R_{EM} from [111, 112].
- The ratio of the Coulomb quadrupole to the magnetic form factor R_{SM} from [111, 112].

For more details see [53]. Since we compare the data with the LCSR predictions, which are expected to work best in the region 1 $\text{GeV}^2 < Q^2 < 10$ GeV^2, we are only interested in experiments where values of the form factors for momentum transfer above $Q^2 = 1$ GeV^2 are available.
For the theory prediction we will use six models (i.e. six determinations for the nonperturbative parameters f_N, λ_1, λ_2, A_1^u, V_1^d, f_1^d, f_1^u and f_2^d) for the nucleon distribution amplitudes including s- and p-wave contributions:

1. QCD sum rule estimates (dotted red lines),
2. asymptotic form (dashed red lines),
3. BLW model (solid red lines),
4. lattice evaluation plus QCD sum rule estimate for f_x^y (dotted blue lines),
5. lattice evaluation plus asymptotic values for f_x^y (dashed blue lines),
6. lattice evaluation plus BLW estimate for f_x^y (solid blue lines).

Since f_1^d, f_1^u and f_2^d have not been determined on the lattice, we have to use in the lattice parameter set QCD sum rule estimates, asymptotic values or the BLW model for f_x^y. For the nucleon form factors we use the LCSRs obtained in [6] and for the $N \to \Delta$ transition we use the LCSRs obtained in [53].
To our accuracy, the sum rules for the nucleon form factors depend only on the five parameters f_N/λ_1, A_1^u, V_1^d, f_1^u and f_1^d. Within the light-cone sum rule approach we determine the form factors F_1 and F_2 directly. The electric and the magnetic form factors G_E and G_M are linear combinations of F_1 and F_2:

$$\begin{aligned} G_M(Q^2) &= F_1(Q^2) + F_2(Q^2)\,, \\ G_E(Q^2) &= F_1(Q^2) - \frac{Q^2}{4m_N^2} F_2(Q^2)\,. \end{aligned} \tag{46}$$

As discussed above, Eq. (46) shows that in G_E cancellations occur. Therefore our predictions for G_E are less reliable than those for G_M.
The light-cone sum rule predictions for the form factors are shown in Figs. 1 - 4. For G_M^p, G_A^p, G_M^n and G_E^n the differences between the lattice determinations and the other approaches (asymptotic, QCD sum rule and BLW) are smaller than the expected overall uncertainties, i.e., the pairs of parameter sets (1) - (4), (2) - (5) and (3) - (6) yield almost identical results. Since f_1^u and f_1^d were chosen to be identical within these pairs, differences can only occur due to V_1^d, A_1^u and f_N/λ_1. The lattice values for V_1^d and A_1^u are very close to the BLW values, while f_N/λ_1 is in the lattice determination about a factor of two smaller than the QCD sum rule estimate. In G_E, $\sqrt{Q^2}F_2^p/((\mu_p - 1)F_1^p)$ and G_T^p cancellations occur, so we expect much bigger theoretical uncertainties and also big differences between our data sets might be possible.
The data for G_M^p (Fig. 1) are very well described with the asymptotic and the BLW data sets, the differences between the parameter sets (2) and (5) and between (3) and (6) are negligible. The pure QCD sum rule estimates (set (1)

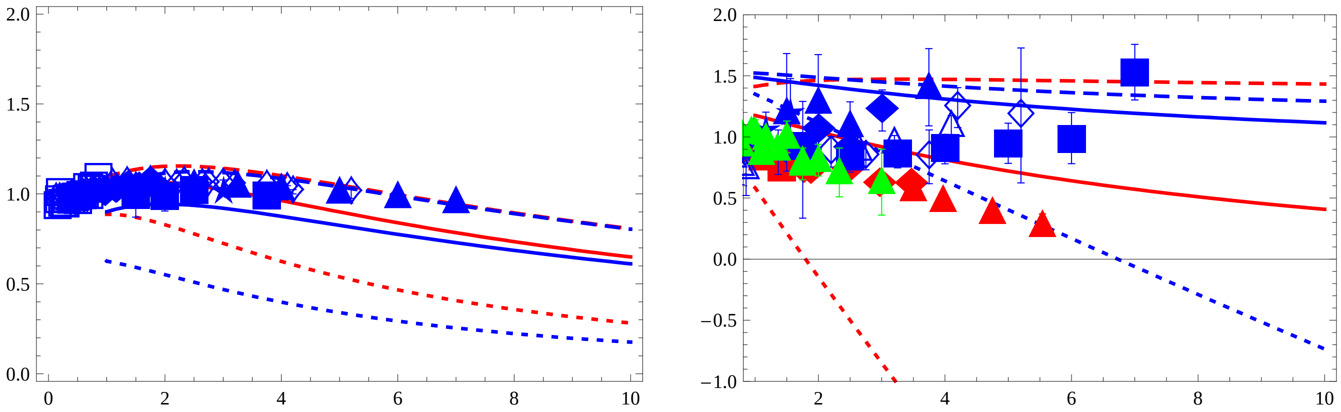

FIG. 1: LCSR results for the electromagnetic form factors (left: $G_M/(\mu_p G_D)$ vs. Q^2; right: $\mu_p G_E/G_M$ vs. Q^2) of the proton, obtained using the BLW model (red solid line), the asymptotic model (red dashed line) and the QCD sum rule model (red dotted line) of the nucleon distribution amplitudes. The corresponding results for the lattice values of the nucleon distribution amplitudes are given in blue. The red data points on the right picture are JLAB data, while the blue and the green ones are obtained via Rosenbluth separation. Currently the Rosenbluth separation data for G_E are judged to be less reliable.

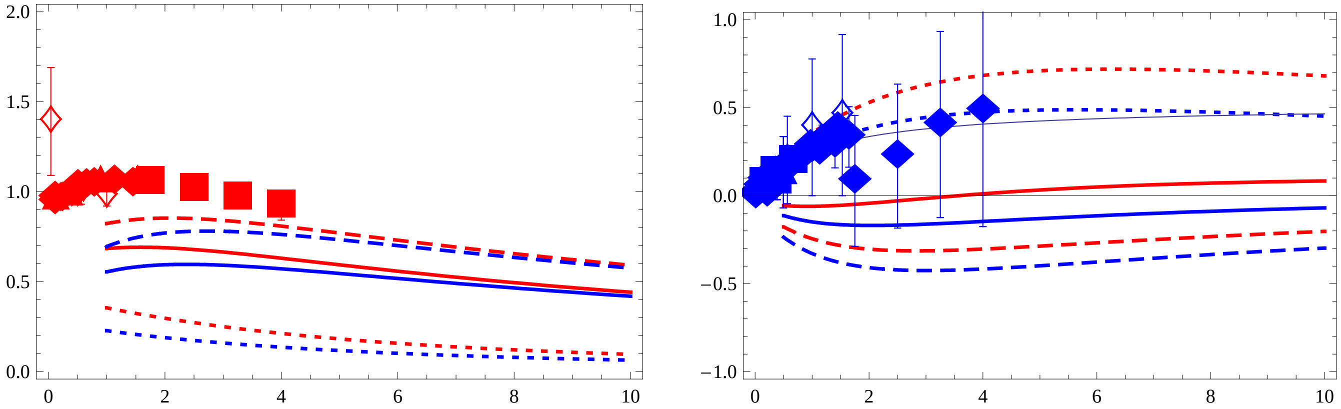

FIG. 2: LCSR results for the electromagnetic form factors of the neutron (left: $G_M/(\mu_n G_D)$ vs. Q^2; right: $G_E/(G_D)$ vs. Q^2), obtained using the BLW model (red solid line), the asymptotic model (red dashed line) and the QCD sum rule model (red dotted line) of the nucleon distribution amplitudes. The corresponding results for the lattice values of the nucleon distribution amplitudes are given in blue. The thin solid blue line represents the updated Galster fit.

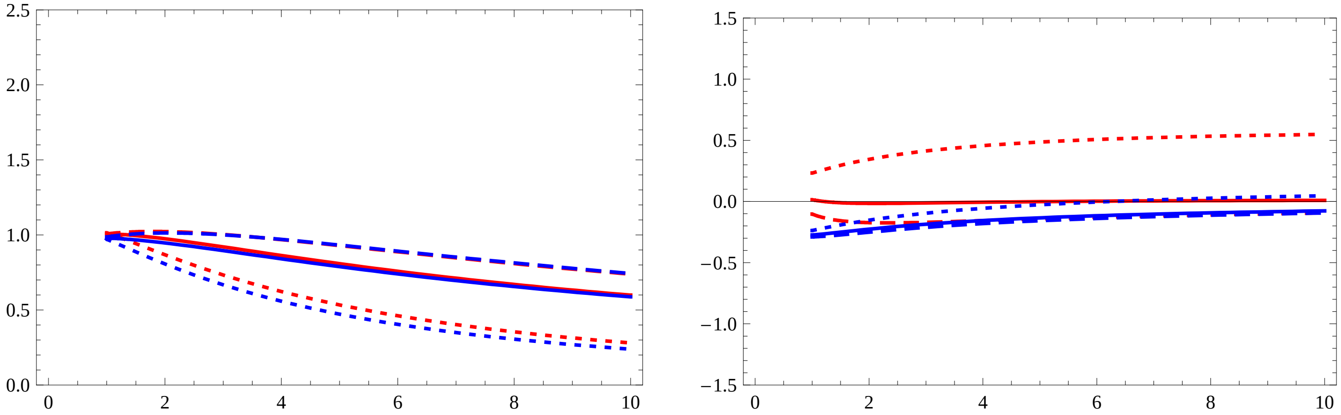

FIG. 3: LCSR results (solid curves) for the axial form factor of the proton G_A normalized to $G_D = g_A/(1+Q^2/m_A^2)^2$ vs. Q^2(left panel) and the tensor form factor G_T normalized to G_A vs. Q^2 (right panel), obtained using the BLW model (red solid line), the asymptotic model (red dashed line) and the QCD sum rule model (red dotted line) of the nucleon distribution amplitudes. The corresponding results for the lattice values of the nucleon distribution amplitudes are given in blue.

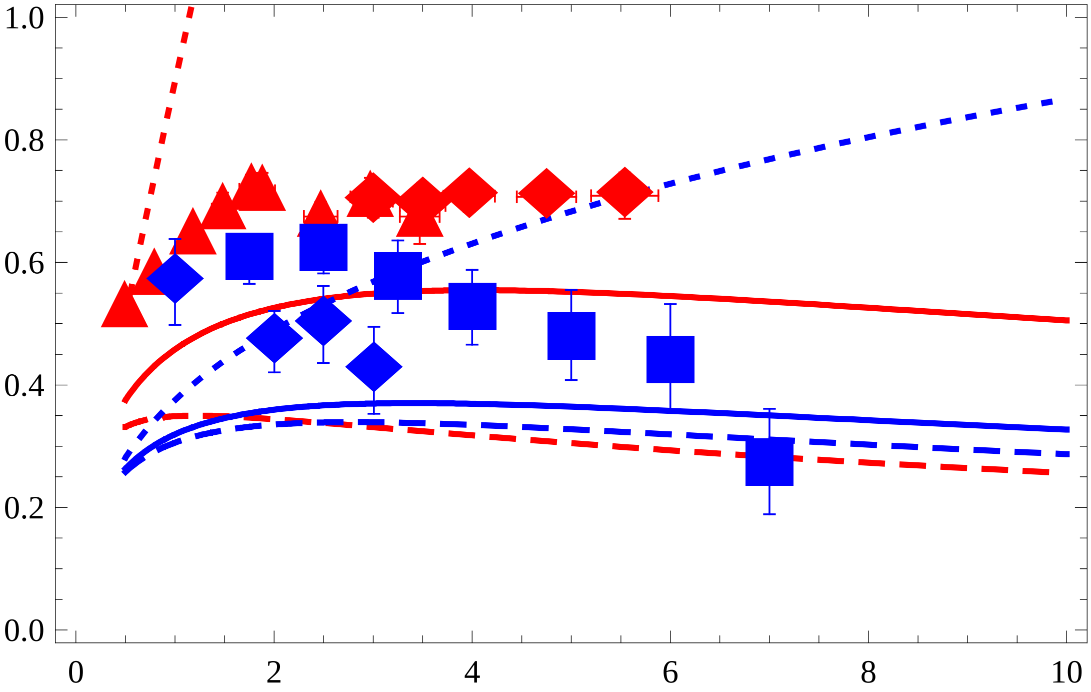

FIG. 4: LCSR results (solid curves) for the ratio $\sqrt{Q^2}F_2^p/(F_1^p * 1.79)$ obtained using the BLW model (solid line), the asymptotic model (dashed line) and the QCD sum rule model (dotted line) of the nucleon distribution amplitudes. The corresponding results for the lattice values of the nucleon distribution amplitudes are given in blue. Red symbols: experimental values obtained via Polarization transfer. Blue symbols: experimental values obtained via Rosenbluth separation. Currently the Rosenbluth separation data for G_E are judged to be less reliable.

and (4)) are about a factor of two too small. In the case of G_M^n (Fig. 2) one sees the same structure for the different models of the nucleon distribution amplitude as for G_M^p, but now all theory predictions are shifted to lower values. For G_A^p (Fig. 3) we agree for Q^2 values below 5 GeV^2 very well with the dipole behavior, if we use the asymptotic or the BLW parameters; for higher Q^2 we predict a slightly steeper fall-off. Again the pure QCD sum rule estimates are considerably worse.

An interesting test of our approach is whether the unphysical tensor form factor G_T (Fig. 3) is consistent with zero. This holds for all parameters sets except the pure QCD sum rule estimates (set (1)). In our approach G_T^p is not exactly zero, because we treat the intial proton state differently from the final proton state: one is described by an interpolating nucleon field, the other by the nucleon distribution amplitude.

Finally we have the ratios G_E^n/G_D (Fig. 2) , G_E^p/G_M^p (Fig. 1), and $\sqrt{Q^2}F_2^p/((\mu_p-1)F_1^p)$ (Fig. 4), which are very sensitive to the explicit form of the nucleon distribution amplitudes due to cancellations in G_E. If we just look at G_E^n our result would be consistent with zero and therefore describes the data well. If we investigate G_E^n/G_D, we blow up the large Q^2 contributions. Now we have a "perfect" agreement between the pure QCD sum rule parameters and the data. Our data set (4) is almost identical to the updated Galster fit. The BLW model is consistent with zero, while the asymptotic distribution amplitude yields negative values. The difference between the lattice values for the distribution amplitudes and the data sets (1) - (3) is visible, but not dramatic. In the case of G_E^p/G_M^p, and $\sqrt{Q^2}F_2^p/(F_1^p * 1.79)$ we can make similar observations. The purely asymptotic values lie above (below) the data for G_E^p/G_M^p ($\sqrt{Q^2}F_2^p/(F_1^p * 1.79)$), the BLW data set moves the results in the right direction, but not far enough. Our data set (1) is completely off, because it predicts a very small value for F_1^p. Now we also have big differences between the lattice values of the distribution amplitudes and the pure QCD sum rule values.

Taking into account that the full $\mathcal{O}(\alpha_s)$-corrections to the LCSRs are not yet available, already a rough agreement of our approach with the data is a success. For G_M^p, G_A^p, G_M^n and G_E^n we get unexpectedly "good" results if we use the BLW form or the asymptotic form of the nucleon distribution amplitude. The corresponding lattice values (set (5) and (6)) give similar results. For G_E^n/G_D, G_E^p/G_M^p, and $\sqrt{Q^2}F_2^p/(F_1^p * 1.79)$ the BLW model lies in the right ball park, but we would prefer a model for the distribution amplitudes which lies in the middle between the asymptotic and the pure QCD sum rule estimate (BLW is closer to the asymptotic value).

In the transition form factors of $\gamma^* N \to \Delta$ all eight non-perturbative parameters appear, see [53]. The results are shown in Fig. 5. As expected, now the differences between the parameter set pairs (1) - (4), (2) - (5) and (3) - (6) are more pronounced. In the case of G_M^* the theory curves generally tend to be more flat than the experimental data. The form factors obtained with the lattice values for the nucleon distribution amplitude lie considerably above the data sets (1) - (3). Above $Q^2 \approx 3$ GeV^2 the asymptotic distribution amplitude and the BLW distribution amplitude are close to the data. The fact that R_{EM} is close to zero is reproduced very well with the BLW parameters (sets (3) and (6)) and the lattice plus asymptotic values (set(5)), while positive values are obtained with the purely asymptotic form (set (2)). One gets a negative result with the QCD sum rule determination of the nucleon distribution amplitude (sets (1) and (4)). In the case of R_{SM} the differences are not very pronounced, all values are close to zero. Altogether one has to conclude that while all approaches give the correct order of magnitude none gives a really convincing description of all data. However in view of the fact that the systematic uncertainities are even more pronounced than for the nucleon form factors more could not have been expected.

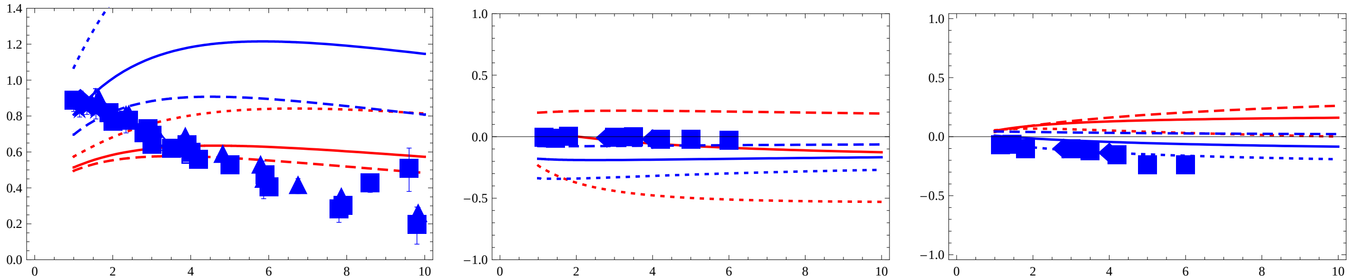

FIG. 5: $\gamma^* N \rightarrow \Delta$ transition form factors (left:$G_M^*/(3G_D)$ vs. Q^2, middle:R_{EM} vs. Q^2, right: R_{SM} vs. Q^2) in the LCSR approach [53] obtained using the BLW model (solid line), the asymptotic model (dashed line) and the QCD sum rule model (dotted line) of the nucleon distribution amplitudes. The corresponding form factors based on the lattice values for the nucleon distribution amplitudes are given in blue.

VIII. REDUCING THE NUMBER OF INDEPENDENT PARAMETERS OF THE DISTRIBUTION AMPLITUDES

In [113] the following approximate relations between twist-4 and twist-3 parameters were derived:

$$\begin{aligned} f_1^d &= \frac{3}{10} - \frac{1}{6}\frac{f_N}{\lambda_1}\,, \\ f_1^u &= \frac{1}{10} - \frac{1}{6}\frac{f_N}{\lambda_1}\,. \end{aligned} \tag{47}$$

Using these relations, we can express the nucleon form factors in terms of only three independent parameters, namely $\frac{f_N}{\lambda_1}$, V_1^d and A_1^u. For the comparison with the data we show now only two models for the remaining three parameters of the nucleon distribution amplitude:

(a) Lattice determination of the distribution amplitude - blue curve.

(b) BLW model - red curve.

We obtain the following values for f_1^x:

	(a)	(b)	asymptotic	BLW	QCD-SR
f_1^u	0.11	0.13	0.10	0.09	0.07
f_1^d	0.31	0.33	0.30	0.33	0.40

which are compared with our previous estimates for f_1^u and f_1^d. In this approach f_1^d lies between the asymptotic and the BLW value; f_1^u is also close to the asymptotic or the BLW value, but its deviation from the asymptotic value is in the "wrong" direction. In Fig. 6 we show the electromagnetic form factors of the proton, in Fig. 7 the electromagnetic form factors of the neutron, in Fig. 8 the axial and the tensor form factor of the proton and finally in Fig. 9 the ratio of the form factors F_2 and F_1 of the proton. In Fig. 10 we show the three $N \rightarrow \Delta$ transition form factors. In all cases we obtain results which are very close the BLW results of the previous section, so it seems that the nucleon form factors are very sensitive to the values of V_1^d and A_1^u, while the dependence on f_N/λ_1, f_1^d and f_1^u is less pronounced.

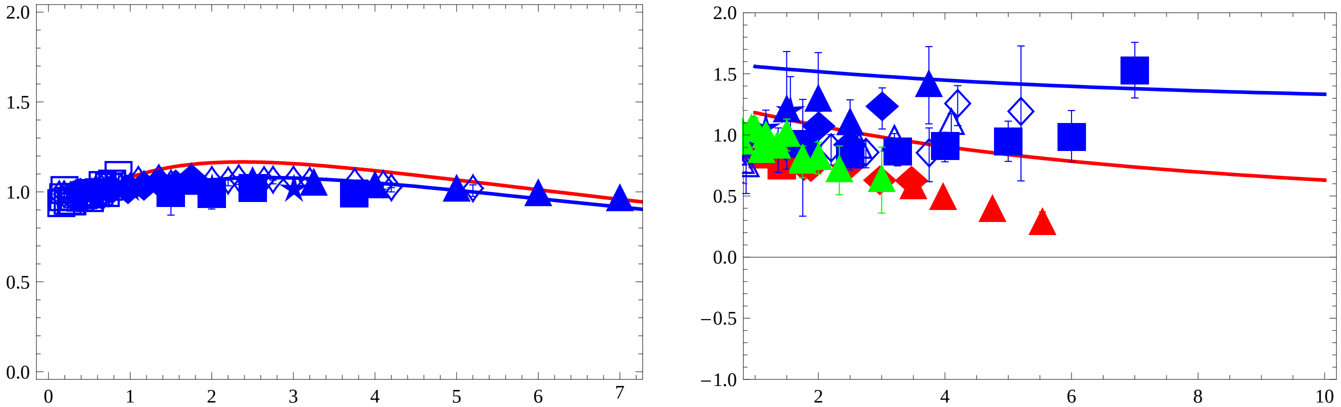

FIG. 6: LCSR results for the electromagnetic form factors (left: $G_M/(\mu_p G_D)$ vs. Q^2; right: $\mu_p G_E/G_M$ vs. Q^2) of the proton, obtained using the BLW model (red solid line) and the lattice prediction (blue solid line) for the nucleon distribution amplitudes. In both cases the parameters f_1^x are determined from the twist-3 parameters, cf. Eq. (47). The red data points on the right picture are JLAB data, while the blue and the green ones are obtained via Rosenbluth separation.

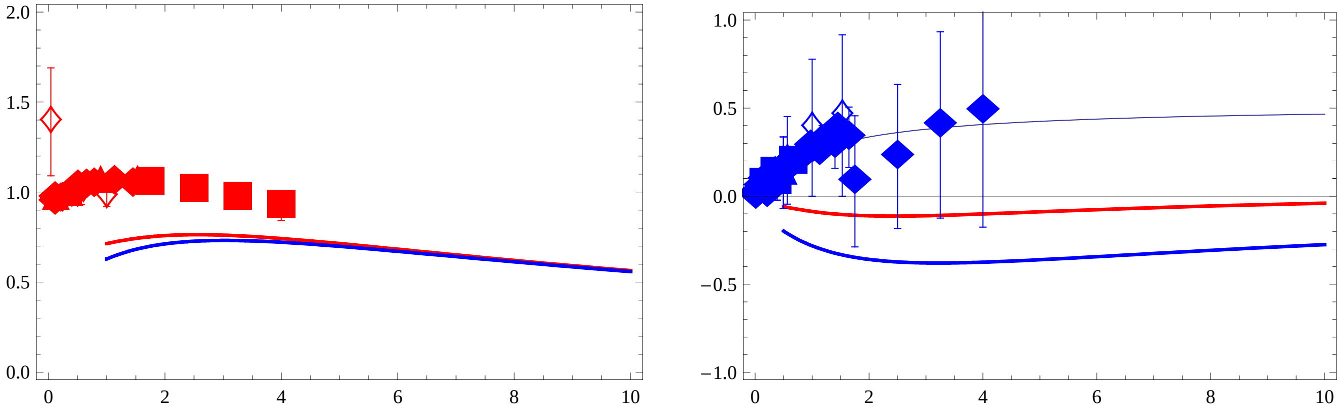

FIG. 7: LCSR results for the electromagnetic form factors of the neutron (left: $G_M/(\mu_n G_D)$ vs. Q^2; right: $G_E/(G_D)$ vs. Q^2), obtained using the BLW model (red solid line) and the lattice prediction (blue solid line) for the nucleon distribution amplitudes. In both cases the parameters f_1^x are determined from the twist-3 parameters, cf. Eq. (47). The thin solid blue line represents the updated Galster fit.

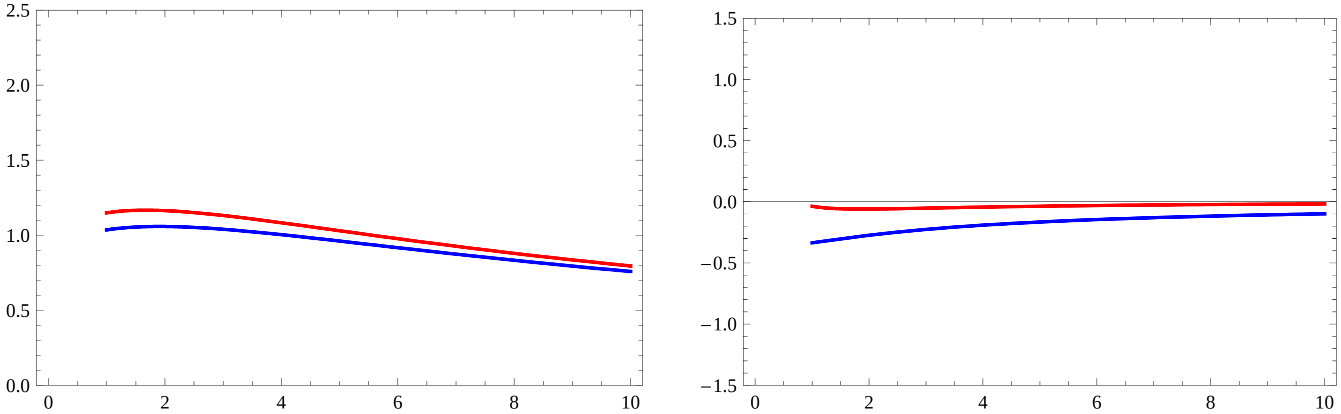

FIG. 8: LCSR results (solid curves) for the axial form factor of the proton G_A normalized to $G_D = g_A/(1+Q^2/m_A^2)^2$ vs. Q^2(left panel) and the tensor form factor G_T normalized to G_A vs. Q^2 (right panel), obtained using the BLW model (red solid line) and the lattice prediction (blue solid line) for the nucleon distribution amplitudes. In both cases the parameters f_1^x are determined from the twist-3 parameters, cf. Eq. (47).

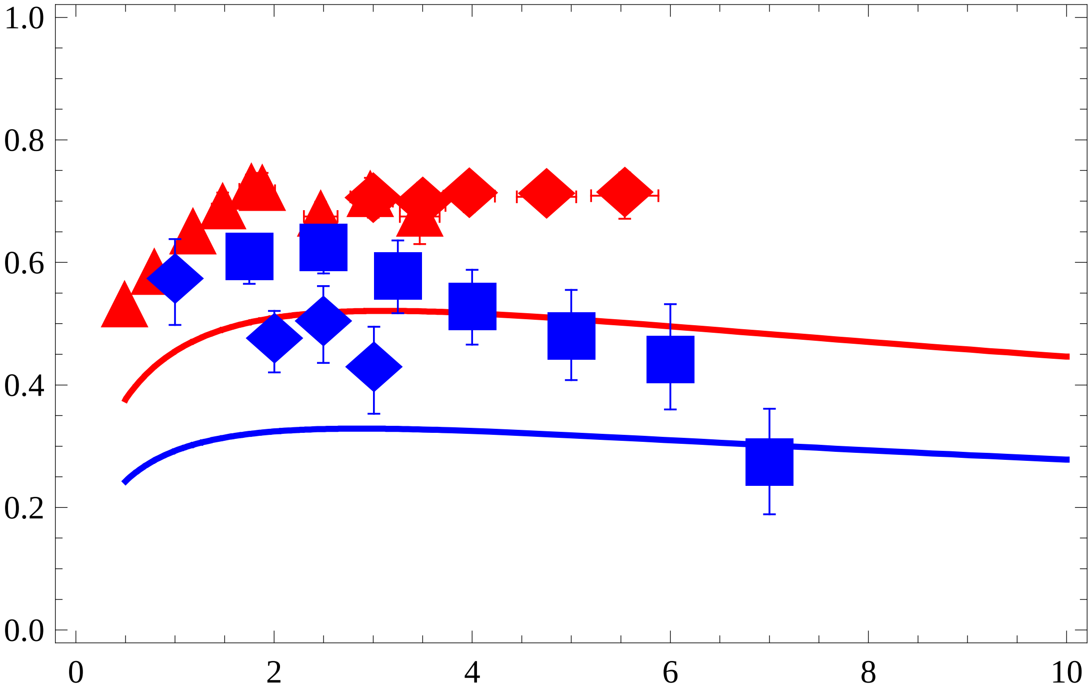

FIG. 9: LCSR results (solid curves) for the ratio $\sqrt{Q^2}F_2^p/(F_1^p * 1.79)$ obtained using the BLW model (red solid line) and the lattice prediction (blue solid line) for the nucleon distribution amplitudes. In both cases the parameters f_1^x are determined from the twist-3 parameters, cf. Eq. (47). Red symbols: experimental values obtained via Polarization transfer. Blue symbols: experimental values obtained via Rosenbluth separation.

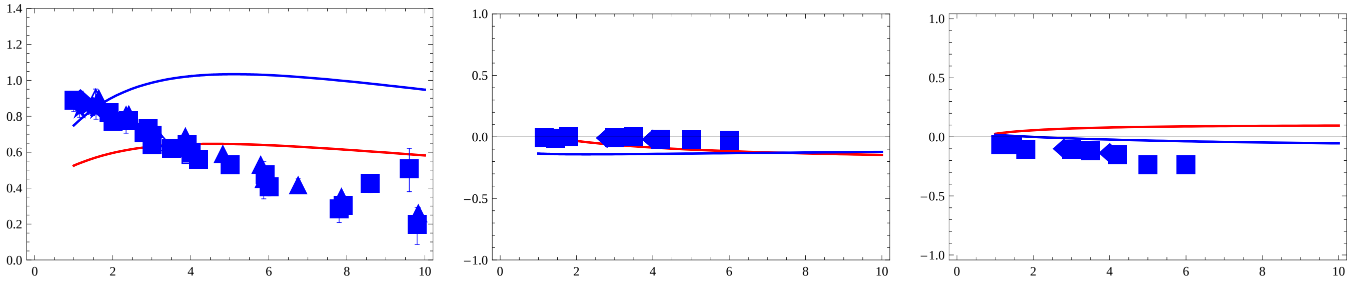

FIG. 10: $\gamma^* N \rightarrow \Delta$ transition form factors (left:$G_M^*/(3G_D)$ vs. Q^2, middle:R_{EM} vs. Q^2, right: R_{SM} vs. Q^2) in the LCSR approach [53] obtained using the BLW model (red solid line) and the lattice prediction (blue solid line) for the nucleon distribution amplitudes. In both cases the parameters f_1^x are determined from the twist-3 parameters, cf. Eq. (47).

IX. EFFECTS OF HIGHER CONFORMAL SPIN CONTRIBUTIONS

In this section we include (in comparison to the previous sections) also contributions of the next-to-next-to leading conformal spin to the leading-twist distribution amplitude. These terms have been determined on the lattice [3, 4] and with QCD sum rules [29, 30, 37]. The explicit expressions for the leading-twist distribution amplitudes can be found in appendix C. The contributions of these higher moments to the electromagnetic form factors of the nucleon have already been estimated in [16], but only for the Chernyak-Zhitnitsky interpolating field. Here we work out the contributions of the second moments to the light-cone sum rules for nucleon form factors using the Ioffe current. We will use the form in Eq. (C1) for the leading-twist distribution amplitude and the following parameter sets:

1. Asymptotic distribution amplitude (black lines).
2. BLW plus second moments from QCD sum rules (dotted red lines).
3. BLW plus second moments from the lattice (dashed red lines).

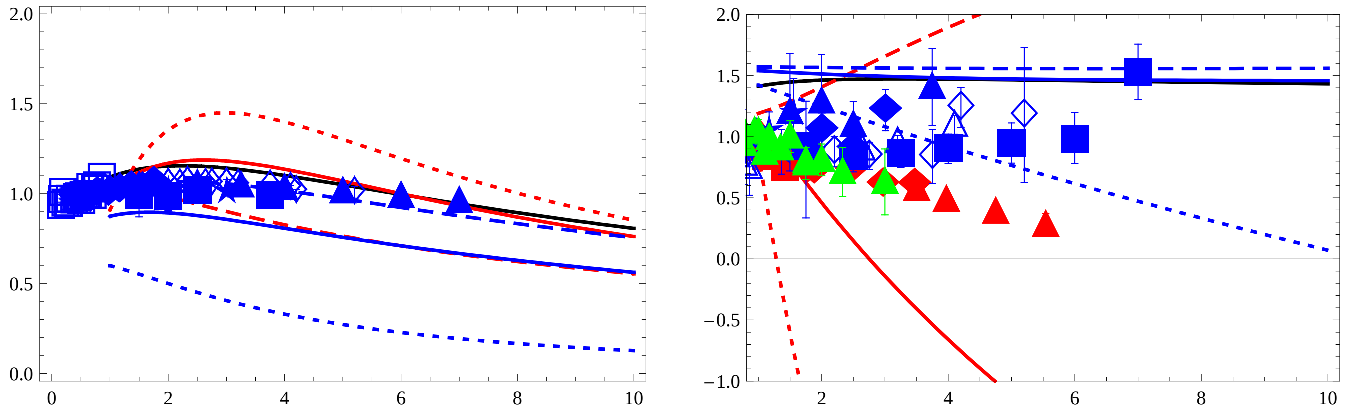

FIG. 11: LCSR results for the electromagnetic form factors (left: $G_M/(\mu_p G_D)$ vs. Q^2; right: $\mu_p G_E/G_M$ vs. Q^2) of the proton, obtained using the asymptotic form (black solid line), the BLW model (red) with second moments from QCD sum rules (dotted), lattice (dashed) and BLW (solid) and the lattice determination (blue) with f_x^y from QCD sum rules (dotted), the asymptotic model (dashed) and the BLW model (solid). The red data points on the right picture are JLAB data, while the blue and green ones are obtained via Rosenbluth separation.

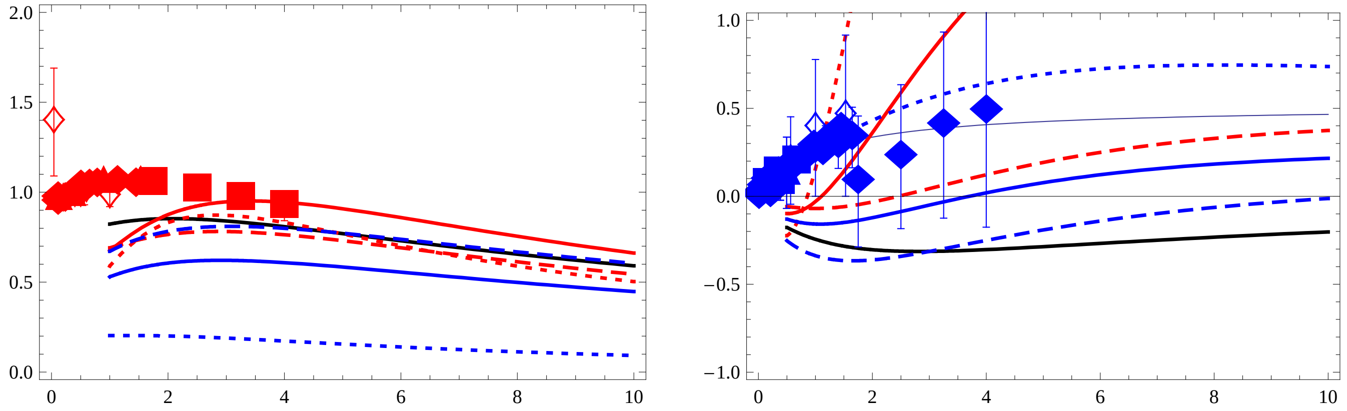

FIG. 12: LCSR results for the electromagnetic form factors of the neutron (left: $G_M/(\mu_n G_D)$ vs. Q^2; right: G_E vs. Q^2), obtained using the asymptotic form (black solid line), the BLW model (red) with second moments from QCD sum rules (dotted), lattice (dashed) and BLW (solid) and the lattice determination (blue) with f_x^y from QCD sum rules (dotted), the asymptotic model (dashed) and the BLW model (solid).

4. BLW plus second moments á la BLW (solid red lines).
5. Lattice evaluation plus QCD sum rule estimates for f_x^y (dotted blue lines).
6. Lattice evaluation plus asymptotic values for f_x^y (dashed blue lines).
7. Lattice evaluation plus BLW estimates for f_x^y (solid blue lines).

In Fig. 11 we show the electromagnetic form factors of the proton, in Fig. 12 the electromagnetic form factors of the neutron, in Fig. 13 the axial and the tensor form factor of the proton and finally in Fig. 14 the ratio of the form factors F_2 and F_1 of the proton. In Fig. 15 we show the three $N \to \Delta$ transition form factors.

In almost all cases the second moments of the leading-twist distribution amplitude determined with QCD sum rules give huge corrections. We show these parameter sets in the plots, but we will not discuss them any further.

The magnetic form factor of the proton G_M^p is very well described by the BLW model with second moments á la BLW (set(4)) or from the lattice (set(3)) and the lattice values for the distribution amplitude with f_x^y from BLW (set (7)) or with the asymptotic values for f_x^y (set (6)). This is not unexpected, since the second moments á la BLW and from the lattice are quite similar in size. This observation ensures, however, that there is not an unexpected strong sensitivity of the LCSRs to the second moments. The theory predictions for the magnetic form factor of the neutron G_M^n are again shifted to lower values. Apart from this fact, the predictions for the parameter sets (1), (3),

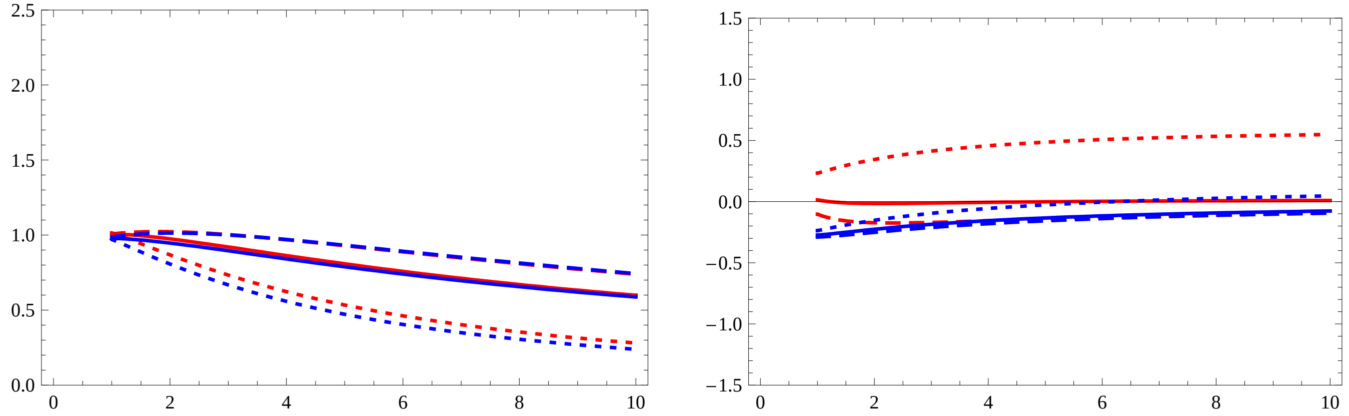

FIG. 13: LCSR results (solid curves) for the axial form factor of the proton G_A normalized to $G_D = g_A/(1+Q^2/m_A^2)^2$ vs. Q^2(left panel) and the tensor form factor G_T normalized to G_A vs. Q^2 (right panel), obtained using the asymptotic form (black solid line), the BLW model (red) with second moments from QCD sum rules (dotted), lattice (dashed) and BLW (solid) and the lattice determination (blue) with f_x^y from QCD sum rules (dotted), the asymptotic model (dashed) and the BLW model (solid).

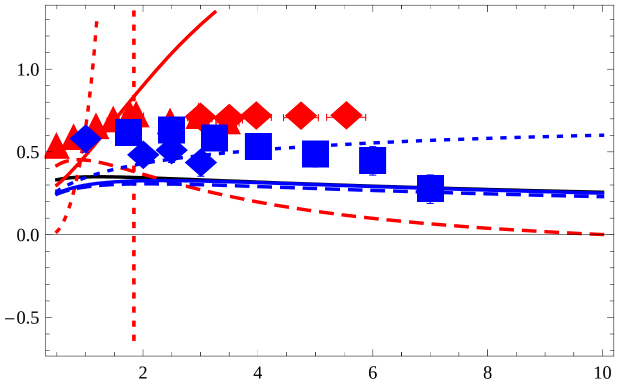

FIG. 14: LCSR results (solid curves) for the ratio $\sqrt{Q^2}F_2^p/(F_1^p * 1.79)$ obtained using the asymptotic form (black solid line), the BLW model (red) with second moments from QCD sum rules (dotted), lattice (dashed) and BLW (solid) and the lattice determination (blue) with f_x^y from QCD sum rules (dotted), the asymptotic model (dashed) and the BLW model (solid). Red symbols: experimental values obtained via Polarization transfer. Blue symbols: experimental values obtained via Rosenbluth separation.

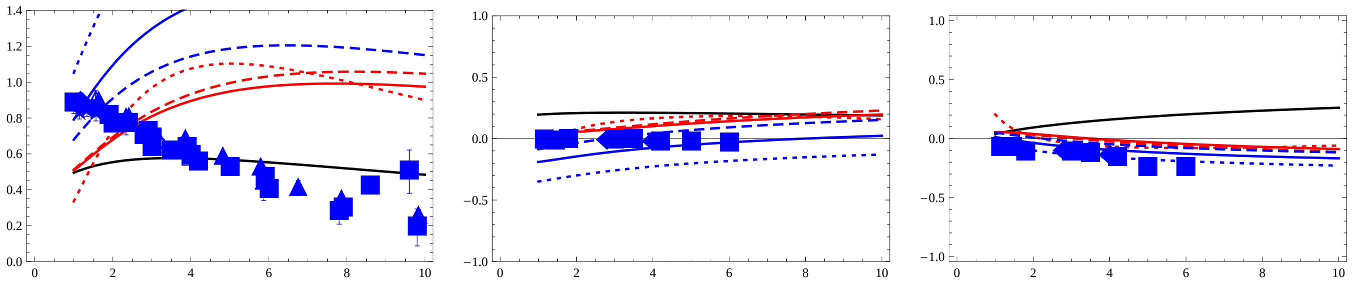

FIG. 15: $\gamma^* N \to \Delta$ transition form factors (left:$G_M^*/(3G_D)$ vs. Q^2, middle:R_{EM} vs. Q^2, right: R_{SM} vs. Q^2) in the LCSR approach [53] obtained using the asymptotic form (black solid line), the BLW model (red) with second moments from QCD sum rules (dotted), lattice (dashed) and BLW (solid) and the lattice determination (blue) with f_x^y from QCD sum rules (dotted), the asymptotic model (dashed) and the BLW model (solid).

(4), (6), (7) lie relatively close together and they agree a little better with experiment, compared to the case where the d-wave contributions have been neglected. Also for G_A^p and G_T^p we get nice results, unless we use the QCD sum rule values of the second moments. As expected, in G_E^p/G_M^p, G_E^n/G_D and F_2^p/F_1^p cancellations arise that lead to a strong dependence on the concrete form of the nucleon distribution amplitudes.
In the case of the $N \to \Delta$ transition the inclusion of d-wave corrections leads to strong enhancements in the prediction of G_M^*, while R_{EM} and R_{SM} agree now better with experiment.

X. CONCLUSION

We have compared a new determination of the nucleon distribution amplitudes based on lattice QCD with different values available in the literature. The non-perturbative parameters of non-leading conformal spin from the lattice evaluation turned out to be close to the asymptotic form and very close to the BLW model. For the leading conformal spin parameters f_N, λ_1 and λ_2 the deviation between lattice and QCD sum rules is about 30%, which is possibly due to neglected radiative corrections in the QCD sum rules estimates. Our models for the nucleon distribution amplitudes can be related to measurable form factors with light-cone sum rules. Despite the fact that the light-cone sum rules are only calculated to leading order in QCD and despite an intrinsic uncertainty of light-cone sum rules of about ±20% we get a very good description of G_M^p, G_M^n, G_A^p and G_T^p at intermediate momentum transfer. In G_E^p, G_E^n and F_2^p/F_1^p cancellations occur, which limit our predictive power. In general we found the following tendency: The asymptotic distribution amplitudes describe the data already amazingly well. Pure QCD sum rule estimates for the non-perturbative parameters overestimate the deviation from the asymptotic form, but the deviation goes in the right direction. The best results are obtained for the BLW values and the very similar lattice values. Including also d-wave contributions to the twist-3 distribution amplitude improves the description of G_M^p, G_M^n, G_A^p and G_T^p a little bit, but results also in bigger uncertainites in G_E^p, G_E^n and F_2^p/F_1^p. In the case of the $N \to \Delta$ transition, we do not see the steep fall-off of G_M^*, but the smallness of R_{EM} and R_{SM} is very well reproduced.
Further improvements on the theoretical side can be achieved by determining the NLO QCD corrections to light-cone sum rules, which connect the nucleon distribution amplitudes to the form factors. To match the NLO QCD accuracy also α_s-corrections have then to be included in all QCD sum rule estimates of the moments of the nucleon distribution amplitudes.

XI. ACKNOWLEDGMENT

We would like to thank V. Braun and A. Schäfer for discussions and comments on the manuscript, R. Schiavilla for providing the data for G_E^n from Ref. [100] and Y. Aoki for clarifying comments. All lattice data were provided by the QCDSF collaboration. This work was supported by DFG (Forschergruppe Gitter-Hadronen-Phänomenologie and SFB/TR55 Hadron Physics from Lattice QCD) and by BMBF.

APPENDIX A: NUCLEON DISTRIBUTION AMPLITUDES UP TO TWIST-6

For completeness we give in this appendix the full expressions for the nucleon distribution amplitudes up to twist-6, details can be found in [2, 6]. The general Lorentz decomposition of the matrix element defined in Eq. (5) reads [2]

$$\begin{aligned}
&4\,\langle 0|\, \epsilon^{ijk} u^i_\alpha(a_1 x) u^j_\beta(a_2 x) d^k_\gamma(a_3 x)\,|P\rangle \\
&= \mathcal{S}_1 m_N C_{\alpha\beta}\left(\gamma_5 N\right)_\gamma + \mathcal{S}_2 m_N^2 C_{\alpha\beta}\left(\not{x}\gamma_5 N\right)_\gamma + \mathcal{P}_1 m_N \left(\gamma_5 C\right)_{\alpha\beta} N_\gamma + \mathcal{P}_2 m_N^2 \left(\gamma_5 C\right)_{\alpha\beta}\left(\not{x} N\right)_\gamma \\
&\quad + \left(\mathcal{V}_1 + \frac{x^2 m_N^2}{4}\mathcal{V}_1^M\right)\left(\not{P} C\right)_{\alpha\beta}\left(\gamma_5 N\right)_\gamma + \mathcal{V}_2 m_N \left(\not{P} C\right)_{\alpha\beta}\left(\not{x}\gamma_5 N\right)_\gamma + \mathcal{V}_3 m_N \left(\gamma_\mu C\right)_{\alpha\beta}\left(\gamma^\mu \gamma_5 N\right)_\gamma \\
&\quad + \mathcal{V}_4 m_N^2 \left(\not{x} C\right)_{\alpha\beta}\left(\gamma_5 N\right)_\gamma + \mathcal{V}_5 m_N^2 \left(\gamma_\mu C\right)_{\alpha\beta}\left(i\sigma^{\mu\nu} x_\nu \gamma_5 N\right)_\gamma + \mathcal{V}_6 m_N^3 \left(\not{x} C\right)_{\alpha\beta}\left(\not{x}\gamma_5 N\right)_\gamma \\
&\quad + \left(\mathcal{A}_1 + \frac{x^2 m_N^2}{4}\mathcal{A}_1^M\right)\left(\not{P}\gamma_5 C\right)_{\alpha\beta} N_\gamma + \mathcal{A}_2 m_N \left(\not{P}\gamma_5 C\right)_{\alpha\beta}\left(\not{x} N\right)_\gamma + \mathcal{A}_3 m_N \left(\gamma_\mu \gamma_5 C\right)_{\alpha\beta}\left(\gamma^\mu N\right)_\gamma \\
&\quad + \mathcal{A}_4 m_N^2 \left(\not{x}\gamma_5 C\right)_{\alpha\beta} N_\gamma + \mathcal{A}_5 m_N^2 \left(\gamma_\mu \gamma_5 C\right)_{\alpha\beta}\left(i\sigma^{\mu\nu} x_\nu N\right)_\gamma + \mathcal{A}_6 m_N^3 \left(\not{x}\gamma_5 C\right)_{\alpha\beta}\left(\not{x} N\right)_\gamma \\
&\quad + \left(\mathcal{T}_1 + \frac{x^2 m_N^2}{4}\mathcal{T}_1^M\right)\left(P^\nu i\sigma_{\mu\nu} C\right)_{\alpha\beta}\left(\gamma^\mu \gamma_5 N\right)_\gamma + \mathcal{T}_2 m_N \left(x^\mu P^\nu i\sigma_{\mu\nu} C\right)_{\alpha\beta}\left(\gamma_5 N\right)_\gamma \\
&\quad + \mathcal{T}_3 m_N \left(\sigma_{\mu\nu} C\right)_{\alpha\beta}\left(\sigma^{\mu\nu}\gamma_5 N\right)_\gamma + \mathcal{T}_4 m_N \left(P^\nu \sigma_{\mu\nu} C\right)_{\alpha\beta}\left(\sigma^{\mu\rho} x_\rho \gamma_5 N\right)_\gamma \\
&\quad + \mathcal{T}_5 m_N^2 \left(x^\nu i\sigma_{\mu\nu} C\right)_{\alpha\beta}\left(\gamma^\mu \gamma_5 N\right)_\gamma + \mathcal{T}_6 m_N^2 \left(x^\mu P^\nu i\sigma_{\mu\nu} C\right)_{\alpha\beta}\left(\not{x}\gamma_5 N\right)_\gamma \\
&\quad + \mathcal{T}_7 m_N^2 \left(\sigma_{\mu\nu} C\right)_{\alpha\beta}\left(\sigma^{\mu\nu}\,\not{x}\gamma_5 N\right)_\gamma + \mathcal{T}_8 m_N^3 \left(x^\nu \sigma_{\mu\nu} C\right)_{\alpha\beta}\left(\sigma^{\mu\rho} x_\rho \gamma_5 N\right)_\gamma \,,
\end{aligned} \tag{A1}$$

with

$$\begin{aligned}
\mathcal{S}_1 &= S_1\,, & 2(P\cdot x)\,\mathcal{S}_2 &= S_1 - S_2\,,\\
\mathcal{P}_1 &= P_1\,, & 2(P\cdot x)\,\mathcal{P}_2 &= P_2 - P_1\,,\\
\mathcal{V}_1 &= V_1\,, & 2(P\cdot x)\,\mathcal{V}_2 &= V_1 - V_2 - V_3\,,\\
2\mathcal{V}_3 &= V_3\,, & 4(P\cdot x)\,\mathcal{V}_4 &= -2V_1 + V_3 + V_4 + 2V_5\,,\\
4(P\cdot x)\mathcal{V}_5 &= V_4 - V_3\,, & 4\,(P\cdot x)^2\,\mathcal{V}_6 &= -V_1 + V_2 + V_3 + V_4 + V_5 - V_6\,,\\
\mathcal{A}_1 &= A_1\,, & 2(P\cdot x)\mathcal{A}_2 &= -A_1 + A_2 - A_3\,,\\
2\mathcal{A}_3 &= A_3\,, & 4(P\cdot x)\mathcal{A}_4 &= -2A_1 - A_3 - A_4 + 2A_5\,,\\
4(P\cdot x)\mathcal{A}_5 &= A_3 - A_4\,, & 4\,(P\cdot x)^2\,\mathcal{A}_6 &= A_1 - A_2 + A_3 + A_4 - A_5 + A_6\,,\\
\mathcal{T}_1 &= T_1\,, & 2(P\cdot x)\mathcal{T}_2 &= T_1 + T_2 - 2T_3\,,\\
2\mathcal{T}_3 &= T_7\,, & 2(P\cdot x)\mathcal{T}_4 &= T_1 - T_2 - 2T_7\,,\\
2(P\cdot x)\mathcal{T}_5 &= -T_1 + T_5 + 2T_8\,, & 4\,(P\cdot x)^2\,\mathcal{T}_6 &= 2T_2 - 2T_3 - 2T_4 + 2T_5 + 2T_7 + 2T_8\,,\\
4(P\cdot x)\mathcal{T}_7 &= T_7 - T_8\,, & 4\,(P\cdot x)^2\,\mathcal{T}_8 &= -T_1 + T_2 + T_5 - T_6 + 2T_7 + 2T_8\,.
\end{aligned} \tag{A2}$$

The calligraphic notation is used for distribution amplitudes belonging to a simple Dirac structure, while the non-calligraphic functions denote distribution amplitudes of definite twist. Each distribution amplitude $F = V_i, A_i, T_i, S_i, P_i$ can be represented as

$$F(a_1, a_2, a_3, (P\cdot x)) = \int \mathcal{D}x\, e^{-i(P\cdot x)\sum_i x_i a_i} F(x_i)\,, \tag{A3}$$

where the functions $F(x_i)$ depend on the dimensionless variables x_i, $0 < x_i < 1, \sum_i x_i = 1$ which correspond to the longitudinal momentum fractions carried by the quarks inside the nucleon.

APPENDIX B: EXPANSION OF THE NUCLEON DISTRIBUTION AMPLITUDES UP TO NEXT-TO LEADING CONFORMAL SPIN

In [2] the distribution amplitudes were expanded up to next-to leading order in the conformal spin. The twist-3 distribution amplitudes read

$$\begin{aligned}
V_1(x_i,\mu) &= 120x_1x_2x_3\left[\phi_3^0(\mu)+\phi_3^+(\mu)(1-3x_3)\right] ,\\
A_1(x_i,\mu) &= 120x_1x_2x_3(x_2-x_1)\phi_3^-(\mu)\,,\\
T_1(x_i,\mu) &= 120x_1x_2x_3\Big[\phi_3^0(\mu)-\frac{1}{2}\left(\phi_3^+-\phi_3^-\right)(\mu)(1-3x_3)\Big]\,.
\end{aligned}\tag{B1}$$

The twist-4 distribution amplitudes read

$$\begin{aligned}
V_2(x_i,\mu) &= 24x_1x_2\left[\phi_4^0(\mu)+\phi_4^+(\mu)(1-5x_3)\right] ,\\
A_2(x_i,\mu) &= 24x_1x_2(x_2-x_1)\phi_4^-(\mu)\,,\\
T_2(x_i,\mu) &= 24x_1x_2\left[\xi_4^0(\mu)+\xi_4^+(\mu)(1-5x_3)\right] ,\\
V_3(x_i,\mu) &= 12x_3\left[\psi_4^0(\mu)(1-x_3)+\psi_4^+(\mu)(1-x_3-10x_1x_2)\right.\\
&\qquad\left.+\psi_4^-(\mu)(x_1^2+x_2^2-x_3(1-x_3))\right] ,\\
A_3(x_i,\mu) &= 12x_3(x_2-x_1)\left[\left(\psi_4^0+\psi_4^+\right)(\mu)+\psi_4^-(\mu)(1-2x_3)\right] ,\\
T_3(x_i,\mu) &= 6x_3\left[(\phi_4^0+\psi_4^0+\xi_4^0)(\mu)(1-x_3)\right.\\
&\qquad+(\phi_4^++\psi_4^++\xi_4^+)(\mu)(1-x_3-10x_1x_2)\\
&\qquad\left.+(\phi_4^--\psi_4^-+\xi_4^-)(\mu)(x_1^2+x_2^2-x_3(1-x_3))\right],\\
T_7(x_i,\mu) &= 6x_3\left[(\phi_4^0+\psi_4^0-\xi_4^0)(\mu)(1-x_3)\right.\\
&\qquad+(\phi_4^++\psi_4^+-\xi_4^+)(\mu)(1-x_3-10x_1x_2)\\
&\qquad\left.+(\phi_4^--\psi_4^--\xi_4^-)(\mu)(x_1^2+x_2^2-x_3(1-x_3))\right],\\
S_1(x_i,\mu) &= 6x_3(x_2-x_1)\left[(\phi_4^0+\psi_4^0+\xi_4^0+\phi_4^++\psi_4^++\xi_4^+)(\mu)\right.\\
&\qquad\qquad\left.+(\phi_4^--\psi_4^-+\xi_4^-)(\mu)(1-2x_3)\right],\\
P_1(x_i,\mu) &= 6x_3(x_1-x_2)\left[(\phi_4^0+\psi_4^0-\xi_4^0+\phi_4^++\psi_4^+-\xi_4^+)(\mu)\right.\\
&\qquad\qquad\left.+(\phi_4^--\psi_4^--\xi_4^-)(\mu)(1-2x_3)\right].
\end{aligned}\tag{B2}$$

The twist-5 amplitudes are given by

$$\begin{aligned}
V_4(x_i,\mu) &= 3\left[\psi_5^0(\mu)(1-x_3)+\psi_5^+(\mu)(1-x_3-2(x_1^2+x_2^2))\right.\\
&\qquad \left.+\,\psi_5^-(\mu)\left(2x_1x_2-x_3(1-x_3)\right)\right],\\
A_4(x_i,\mu) &= 3(x_2-x_1)\left[-\psi_5^0(\mu)+\psi_5^+(\mu)(1-2x_3)+\psi_5^-(\mu)x_3\right],\\
T_4(x_i,\mu) &= \frac{3}{2}\left[(\phi_5^0+\psi_5^0+\xi_5^0)(\mu)(1-x_3)\right.\\
&\qquad +\left(\phi_5^++\psi_5^++\xi_5^+\right)(\mu)(1-x_3-2(x_1^2+x_2^2))\\
&\qquad \left.+\left(\phi_5^--\psi_5^-+\xi_5^-\right)(\mu)\left(2x_1x_2-x_3(1-x_3)\right)\right],\\
T_8(x_i,\mu) &= \frac{3}{2}\left[(\phi_5^0+\psi_5^0-\xi_5^0)(\mu)(1-x_3)\right.\\
&\qquad +\left(\phi_5^++\psi_5^+-\xi_5^+\right)(\mu)(1-x_3-2(x_1^2+x_2^2))\\
&\qquad \left.+\left(\phi_5^--\psi_5^--\xi_5^-\right)(\mu)\left(2x_1x_2-x_3(1-x_3)\right)\right],\\
V_5(x_i,\mu) &= 6x_3\left[\phi_5^0(\mu)+\phi_5^+(\mu)(1-2x_3)\right],\\
A_5(x_i,\mu) &= 6x_3(x_2-x_1)\phi_5^-(\mu),\\
T_5(x_i,\mu) &= 6x_3\left[\xi_5^0(\mu)+\xi_5^+(\mu)(1-2x_3)\right],\\
S_2(x_i,\mu) &= \frac{3}{2}(x_2-x_1)\left[-\left(\phi_5^0+\psi_5^0+\xi_5^0\right)(\mu)\right.\\
&\qquad +\left(\phi_5^++\psi_5^++\xi_5^+\right)(\mu)(1-2x_3)\\
&\qquad \left.+\left(\phi_5^--\psi_5^-+\xi_5^-\right)(\mu)x_3\right],\\
P_2(x_i,\mu) &= \frac{3}{2}(x_2-x_1)\left[-\left(-\phi_5^0-\psi_5^0+\xi_5^0\right)(\mu)\right.\\
&\qquad +\left(-\phi_5^+-\psi_5^++\xi_5^+\right)(\mu)(1-2x_3)\\
&\qquad \left.+\left(-\phi_5^-+\psi_5^-+\xi_5^-\right)(\mu)x_3\right],
\end{aligned}\tag{B3}$$

and the twist-6 contributions are given by

$$\begin{aligned}
V_6(x_i,\mu) &= 2\left[\phi_6^0(\mu)+\phi_6^+(\mu)(1-3x_3)\right],\\
A_6(x_i,\mu) &= 2(x_2-x_1)\phi_6^-,\\
T_6(x_i,\mu) &= 2\Big[\phi_6^0(\mu)-\frac{1}{2}\left(\phi_6^+-\phi_6^-\right)(1-3x_3)\Big].
\end{aligned}\tag{B4}$$

The coefficients ϕ_i^x, ψ_i^x and ξ_i^x (i stands for the twist) in the above expansions can be expressed in terms of the eight non-perturbative parameters $f_N, \lambda_1, \lambda_2, f_1^u, f_1^d, f_2^d, A_1^u, V_1^d$, defined in section 2. The corresponding relations read, for the leading conformal spin:

$$\begin{aligned}
&\phi_3^0=\phi_6^0=f_N\,, \qquad \phi_4^0=\phi_5^0=\frac{1}{2}\left(f_N+\lambda_1\right),\\
&\xi_4^0=\xi_5^0=\frac{1}{6}\lambda_2\,, \qquad \psi_4^0=\psi_5^0=\frac{1}{2}\left(f_N-\lambda_1\right).
\end{aligned}\tag{B5}$$

For the next-to-leading spin, for twist-3:

$$\phi_3^-=\frac{21}{2}f_N\,A_1^u, \qquad \phi_3^+=\frac{7}{2}f_N\,(1-3V_1^d),\tag{B6}$$

for twist-4:

$$\begin{aligned}
\phi_4^+ &= \frac{1}{4}\left[f_N(3-10V_1^d)+\lambda_1(3-10f_1^d)\right],\\
\phi_4^- &= -\frac{5}{4}\left[f_N(1-2A_1^u)-\lambda_1(1-2f_1^d-4f_1^u)\right],\\
\psi_4^+ &= -\frac{1}{4}\left[f_N(2+5A_1^u-5V_1^d)-\lambda_1(2-5f_1^d-5f_1^u)\right],\\
\psi_4^- &= \frac{5}{4}\left[f_N(2-A_1^u-3V_1^d)-\lambda_1(2-7f_1^d+f_1^u)\right],\\
\xi_4^+ &= \frac{1}{16}\lambda_2(4-15f_2^d)\,,\ \ \xi_4^-=\frac{5}{16}\lambda_2(4-15f_2^d),
\end{aligned}\tag{B7}$$

for twist-5:

$$
\begin{aligned}
\phi_5^+ &= -\frac{5}{6}\left[f_N(3+4V_1^d)-\lambda_1(1-4f_1^d)\right], \\
\phi_5^- &= -\frac{5}{3}\left[f_N(1-2A_1^u)-\lambda_1(f_1^d-f_1^u)\right], \\
\psi_5^+ &= -\frac{5}{6}\left[f_N(5+2A_1^u-2V_1^d)-\lambda_1(1-2f_1^d-2f_1^u)\right], \\
\psi_5^- &= \frac{5}{3}\left[f_N(2-A_1^u-3V_1^d)+\lambda_1(f_1^d-f_1^u)\right], \\
\xi_5^+ &= \frac{5}{36}\lambda_2(2-9f_2^d), \quad \xi_5^- = -\frac{5}{4}\lambda_2 f_2^d,
\end{aligned}
\tag{B8}
$$

and for twist-6:

$$
\begin{aligned}
\phi_6^+ &= \frac{1}{2}\left[f_N(1-4V_1^d)-\lambda_1(1-2f_1^d)\right], \\
\phi_6^- &= \frac{1}{2}\left[f_N(1+4A_1^u)+\lambda_1(1-4f_1^d-2f_1^u)\right].
\end{aligned}
\tag{B9}
$$

x^2-corrections:

Next we summarize the expressions for the x^2-corrections to the leading twist distribution amplitudes V_1, A_1 and T_1. These corrections have been determined in [6, 16, 27, 28].
For V_1 we have

$$
\begin{aligned}
\mathcal{V}_1^{M(u)}(x_2) &= \int_0^{1-x_2} dx_1 V_1^M(x_1,x_2,1-x_1-x_2) = \frac{x_2^2}{24}\left(f_N C_f^u+\lambda_1 C_\lambda^u\right), \\
\mathcal{V}_1^{M(d)}(x_3) &= \int_0^{1-x_3} dx_1 V_1^M(x_1,1-x_1-x_3,x_3) = \frac{x_3^2}{24}\left(f_N C_f^d+\lambda_1 C_\lambda^d\right)
\end{aligned}
\tag{B10}
$$

with

$$
\begin{aligned}
C_f^u &= (1-x_2)^3\left[113+495x_2-552x_2^2-10A_1^u(1-3x_2)+2V_1^d(113-951x_2+828x_2^2)\right], \\
C_\lambda^u &= -(1-x_2)^3\left[13-20f_1^d+3x_2+10f_1^u(1-3x_2)\right], \\
C_f^d &= -(1-x_3)\big[1441+505x_3-3371x_3^2+3405x_3^3-1104x_3^4 \\
&\quad -24V_1^d\big(207-3x_3-368x_3^2+412x_3^3-138x_3^4\big)\big]-12(73-220V_1^d)\ln(x_3), \\
C_\lambda^d &= -(1-x_3)\Big[11+131x_3-169x_3^2+63x_3^3-30f_1^d(3+11x_3-17x_3^2+7x_3^3)\Big] \\
&\quad -12(3-10f_1^d)\ln(x_3).
\end{aligned}
\tag{B11}
$$

In the case of A_1 one finds

$$
\begin{aligned}
\mathcal{A}_1^{M(u)}(x_2) &= \int_0^{1-x_2} dx_1 A_1^M(x_1,x_2,1-x_1-x_2) = \frac{x_2^2}{24}(1-x_2)^3\left(f_N D_f^u+\lambda_1 D_\lambda^u\right), \\
\mathcal{A}_1^{M(d)}(x_3) &= \int_0^{1-x_3} dx_1 A_1^M(x_1,1-x_1-x_3,x_3) = 0,
\end{aligned}
\tag{B12}
$$

with

$$
\begin{aligned}
D_f^u &= 11+45x_2-2A_1^u(113-951x_2+828x_2^2)+10V_1^d(1-30x_2), \\
D_\lambda^u &= 29-45x_2-10f_1^u(7-9x_2)-20f_1^d(5-6x_2).
\end{aligned}
\tag{B13}
$$

Finally, for T_1 one has

$$\begin{aligned}
\mathcal{T}_1^{M(u)}(x_2) &= \int\limits_0^{1-x_2} dx_1 T_1^M(x_1, x_2, 1-x_1-x_2) = \frac{x_2^2}{48}\left(f_N E_f^u + \lambda_1 E_\lambda^u\right), \\
\mathcal{T}_1^{M(d)}(x_3) &= \int\limits_0^{1-x_3} dx_1 T_1^M(x_1, 1-x_1-x_3, x_3) = \frac{x_3^2(1-x_3)^4}{4}\left(f_N E_f^d + \lambda_1 E_\lambda^d\right)
\end{aligned} \tag{B14}$$

with

$$\begin{aligned}
E_f^u &= -\Big[(1-x_2)\left(3(439+71x_2-621x_2^2+587x_2^3-184x_2^4)\right. \\
&\quad \left. + 4A_1^u(1-x_2)^2(59-483x_2+414x_2^2) - 4V_1^d(1301-619x_2-769x_2^2+1161x_2^3-414x_2^4)\right)\Big] \\
&\quad - 12(73-220V_1^d)\ln(x_2)\,, \\
E_\lambda^u &= -\Big[(1-x_2)(5-211x_2+281x_2^2-111x_2^3 \\
&\quad + 10(1+61x_2-83x_2^2+33x_2^3)f_1^d - 40(1-x_2)^2(2-3x_2)f_1^u)\Big] - 12(3-10f_1^d)\ln(x_2)\,, \\
E_f^d &= 17+92x_3+12(A_1^u+V_1^d)(3-23x_3)\,, \\
E_\lambda^d &= -7+20f_1^d+10f_1^u\,.
\end{aligned} \tag{B15}$$

APPENDIX C: EXPANSION OF THE NUCLEON DISTRIBUTION AMPLITUDE OF TWIST-3 UP TO NEXT-TO-NEXT-TO LEADING CONFORMAL SPIN

The expansion of the leading-twist distribution amplitude in a basis which is diagonal with respect to one-loop renormalization reads up to next-to-next-to-leading conformal spin

$$\begin{aligned}
\varphi(x_1, x_2, x_3, \mu) = 120x_1x_2x_3 f_N(\mu_0) L^{\frac{2}{3\beta_0}} \Big\{ & 1 + h_{10}(\mu_0)(x_1 - 2x_2 + x_3) L^{\frac{8}{3\beta_0}} \\
& + h_{11}(\mu_0)(x_1 - x_3) L^{\frac{20}{9\beta_0}} \\
& + h_{20}(\mu_0)\left[1 + 7(x_2 - 2x_1x_3 - 2x_2^2)\right] L^{\frac{14}{3\beta_0}} \\
& + h_{21}(\mu_0)\,(1-4x_2)\,(x_1-x_3)\, L^{\frac{40}{9\beta_0}} \\
& + h_{22}(\mu_0)\left[3 - 9x_2 + 8x_2^2 - 12x_1x_3\right] L^{\frac{32}{9\beta_0}} \Big\}
\end{aligned} \tag{C1}$$

with

$$L = \frac{\alpha_s(\mu)}{\alpha_s(\mu_0)}\,, \qquad \beta_0 = 11 - \frac{2}{3}n_F\,. \tag{C2}$$

The coefficients h_{ij} can be expressed in terms of the moments by

$$h_{10}(\mu) = \frac{7}{2}\left(1 - 3\varphi^{010}(\mu)\right) \tag{C3}$$

$$= -\frac{7}{4}\left(1 - 3\left(A_1^u(\mu) + V_1^d(\mu)\right)\right) \tag{C4}$$

$$= -\frac{1}{2}\left(\tilde{\phi}_3^+(\mu) - \tilde{\phi}_3^-(\mu)\right) , \tag{C5}$$

$$h_{11}(\mu) = \frac{21}{2}\left(\varphi^{100}(\mu) - \varphi^{001}(\mu)\right) \tag{C6}$$

$$= \frac{21}{4}\left(1 + A_1^u(\mu) - 3V_1^d(\mu)\right) \tag{C7}$$

$$= \frac{1}{2}\left(3\tilde{\phi}_3^+(\mu) + \tilde{\phi}_3^-(\mu)\right) , \tag{C8}$$

$$h_{20}(\mu) = \frac{18}{5}\left(h_{10}(\mu) + 4 - 7\left(3\varphi^{101}(\mu) + \varphi^{200}(\mu) + \varphi^{002}(\mu)\right)\right) , \tag{C9}$$

$$h_{21}(\mu) = 126\left(\varphi^{200}(\mu) - \varphi^{002}(\mu)\right) - 9h_{11}(\mu) , \tag{C10}$$

$$h_{22}(\mu) = \frac{21}{5}\left(-h_{10}(\mu) - 4 + 6\left(\varphi^{101}(\mu) + 2\varphi^{200}(\mu) + 2\varphi^{002}(\mu)\right)\right) . \tag{C11}$$

Of course, this form of φ is not uniquely determined by the moments. The anomalous dimensions were obtained, e.g., in [114, 115, 116].
One can also write down the renormalization group equations for the moments $\varphi^{n_1 n_2 n_3} = V_1^{n_1 n_2 n_3} - A_1^{n_1 n_2 n_3}$ alone:

$$\varphi^{100}(\mu) = \frac{1}{21}\left(7 + h_{10}(\mu_0)L^{\frac{8}{3\beta_0}} + h_{11}(\mu_0)L^{\frac{20}{9\beta_0}}\right) , \tag{C12}$$

$$\varphi^{010}(\mu) = \frac{1}{21}\left(7 - 2h_{10}(\mu_0)L^{\frac{8}{3\beta_0}}\right) , \tag{C13}$$

$$\varphi^{001}(\mu) = \frac{1}{21}\left(7 + h_{10}(\mu_0)L^{\frac{8}{3\beta_0}} - h_{11}(\mu_0)L^{\frac{20}{9\beta_0}}\right) , \tag{C14}$$

$$\varphi^{101}(\mu) = \frac{1}{126}\left(12 + 3h_{10}(\mu_0)L^{\frac{8}{3\beta_0}} - 2h_{20}(\mu_0)L^{\frac{14}{3\beta_0}} - h_{22}(\mu_0)L^{\frac{32}{9\beta_0}}\right) , \tag{C15}$$

$$\begin{aligned}\varphi^{200}(\mu) = \frac{1}{252}\Big(&36 + 9h_{10}(\mu_0)L^{\frac{8}{3\beta_0}} + 9h_{11}(\mu_0)L^{\frac{20}{9\beta_0}} \\ &+h_{20}(\mu_0)L^{\frac{14}{3\beta_0}} + h_{21}(\mu_0)L^{\frac{40}{9\beta_0}} + 3h_{22}(\mu_0)L^{\frac{32}{9\beta_0}}\Big) ,\end{aligned} \tag{C16}$$

$$\begin{aligned}\varphi^{002}(\mu) = \frac{1}{252}\Big(&36 + 9h_{10}(\mu_0)L^{\frac{8}{3\beta_0}} - 9h_{11}(\mu_0)L^{\frac{20}{9\beta_0}} \\ &+h_{20}(\mu_0)L^{\frac{14}{3\beta_0}} - h_{21}(\mu_0)L^{\frac{40}{9\beta_0}} + 3h_{22}(\mu_0)L^{\frac{32}{9\beta_0}}\Big) .\end{aligned} \tag{C17}$$

Next we determine V_1, A_1 and T_1 from φ up to d-wave contributions. Including all anomalous dimensions we obtain (in the following we suppress the explicit renormalization scale dependence in the formulas)

$$\begin{aligned}V_1(x_1,x_2,x_3) = 120x_1x_2x_3 f_N L^{\frac{2}{3\beta_0}} \Big\{&1 - \frac{h_{10}}{2}(1-3x_3)L^{\frac{8}{3\beta_0}} + \frac{h_{11}}{2}(1-3x_3)L^{\frac{20}{9\beta_0}} \\ &- \frac{h_{20}}{2}\left[(-2 + 7(x_1 + x_2 - 4x_1x_2)\right] L^{\frac{14}{3\beta_0}} \\ &- \frac{h_{21}}{2}\left[-1 + 8x_2 - 8x_2^2 - x_3 - 8x_2x_3 + 4x_3^2\right] L^{\frac{40}{9\beta_0}} \\ &+ \frac{h_{22}}{2}\left[6 - 21x_1 + 20x_1^2 - 21x_2 + 24x_1x_2 + 20x_2^2\right] L^{\frac{32}{9\beta_0}}\Big\} ,\end{aligned} \tag{C18}$$

$$\begin{aligned}A_1(x_1,x_2,x_3) = -60x_1x_2x_3(x_1-x_2) f_N L^{\frac{2}{3\beta_0}} \Big\{&3h_{10}L^{\frac{8}{3\beta_0}} + h_{11}L^{\frac{20}{9\beta_0}} \\ &+(1-4x_3)\left(7h_{20}L^{\frac{14}{3\beta_0}} + h_{21}L^{\frac{40}{9\beta_0}} + h_{22}L^{\frac{32}{9\beta_0}}\right)\Big\} ,\end{aligned} \tag{C19}$$

$$
\begin{aligned}
T_1(x_1,x_2,x_3) = 120 x_1 x_2 x_3 f_N L^{\frac{2}{3\beta_0}} \Big\{ 1 &+ h_{10}(1-3x_3) L^{\frac{8}{3\beta_0}} \\
&- h_{20}\left[-1+14x_1x_2-7x_3+14x_3^2\right] L^{\frac{14}{3\beta_0}} \\
&- h_{22}\left[-3+12x_1x_2+9x_3-8x_3^2\right] L^{\frac{32}{9\beta_0}} \Big\} \,. \qquad \text{(C20)}
\end{aligned}
$$

In the light-cone sum rule determination of the nucleon form factors we need the distribution amplitudes at a certain renormalization scale $\mu = \mu_0$, therefore we give also the simplified expressions ($L \equiv 1$) in the following.
Our expressions agree up to next-to-leading conformal spin with the correspondings ones of [2]. In [16] the vector function V_1 including the next-to-next-to-leading conformal spin was used with the following notation:

$$
\begin{aligned}
V_1(x_1,x_2,x_3) = 120 x_1 x_2 x_3 f_N \Big[1 &+ \tilde{\phi}_3^{+}(\mu)(1-3x_3) + \tilde{\phi}_3^{d1}\left[3-21x_3+28x_3^2\right] \\
&+ \tilde{\phi}_3^{d2}\left[5(x_1^2+x_2^2)-3(1-x_3)^2)\right] \Big] \,, \qquad \text{(C21)}
\end{aligned}
$$

$$
A_1(x_1,x_2,x_3) = 120 x_1 x_2 x_3 (x_2-x_1) f_N \left\{ \tilde{\phi}_3^{-} + (1-4x_3)\tilde{\phi}_3^{d3} \right\} \,, \qquad \text{(C22)}
$$

$$
\begin{aligned}
T_1(x_1,x_2,x_3,\mu) = 120 x_1 x_2 x_3 f_N \Big\{ 1 &+ \frac{1}{2}(\tilde{\phi}_3^{-} - \tilde{\phi}_3^{+})(1-3x_3) \\
&+ \tilde{\phi}_3^{d4}\left[1-14x_1x_2+7x_3-14x_3^2\right] \\
&+ \tilde{\phi}_3^{d5}\left[1+x_1x_2-8x_3+11x_3^2\right] \Big\} \,, \qquad \text{(C23)}
\end{aligned}
$$

with

$$
\begin{aligned}
\tilde{\phi}_3^{d1} &= \frac{1}{10}\left(h_{20}-h_{21}+3h_{22}\right) && \text{(C24)} \\
&= \frac{9}{10}\left(3+28\varphi^{002}-21V_1^d\right) \,, && \text{(C25)} \\
\tilde{\phi}_3^{d2} &= \frac{1}{5}\left(-7h_{20}+2h_{21}+4h_{22}\right) && \text{(C26)} \\
&= -\frac{63}{5}\left(3+5A_1^u-V_1^d-2(\varphi^{002}+5\varphi^{101}+5\varphi^{200})\right) \,, && \text{(C27)} \\
\tilde{\phi}_3^{d3} &= \frac{1}{2}\left(7h_{20}+h_{21}+h_{22}\right) && \text{(C28)} \\
&= \frac{63}{2}\left(A_1^u+4V_1^d-4(\varphi^{002}+2\varphi^{101})\right) \,, && \text{(C29)} \\
\tilde{\phi}_3^{d4} &= h_{20}+h_{22} && \text{(C30)} \\
&= -\frac{9}{20}\left(3+7(A_1^u+V_1^d)-56(\varphi^{002}-2\varphi^{101}+\varphi^{200})\right) \,, && \text{(C31)} \\
\tilde{\phi}_3^{d5} &= 2h_{22} && \text{(C32)} \\
&= -\frac{63}{10}\left(3+7(A_1^u+V_1^d)-8(2\varphi^{002}+\varphi^{101}+2\varphi^{200})\right) \,. && \text{(C33)}
\end{aligned}
$$

Numerically one obtains for the COZ model [30]

$$
\begin{aligned}
\tilde{\phi}_3^{d1}(\mu = 1\text{GeV}) &= 0.61 \,, && \text{(C34)} \\
\tilde{\phi}_3^{d2}(\mu = 1\text{GeV}) &= 3.7 \,. && \text{(C35)}
\end{aligned}
$$

This agrees with the numbers quoted in [16]. Using the lattice calculation we get

$$
\begin{aligned}
\tilde{\phi}_3^{d1}(\mu = 1\text{GeV}) &= 0.51 \,, && \text{(C36)} \\
\tilde{\phi}_3^{d2}(\mu = 1\text{GeV}) &= 0.71 \,. && \text{(C37)}
\end{aligned}
$$

Here again the pure QCD sum rule calculation seems to overstimate the effects.

APPENDIX D: MODELS FOR THE LEADING-TWIST NUCLEON DISTRIBUTION AMPLITUDE

In this section we present concrete models for the leading-twist nucleon distribution amplitude including next-to-next-to-leading conformal spin at the renormalization scale 1 GeV. At twist-3 one independent distribution amplitude $\varphi(x_1, x_2, x_3, \mu)$ arises, see, e.g., [2]:

$$\varphi(x_1, x_2, x_3, \mu) = (V_1 - A_1)(x_1, x_2, x_3, \mu) \,. \tag{D1}$$

In [2] this distribution amplitude was denoted by $\Phi_3(x_1, x_2, x_3, \mu)$. From φ one easily gets V_1, A_1 and T_1, see, e.g., [2]:

$$\begin{aligned} T_1(x_1, x_2, x_3) &= \frac{1}{2}\left[\varphi(x_1, x_3, x_2) + \varphi(x_2, x_3, x_1)\right] \,, & \text{(D2)} \\ V_1(x_1, x_2, x_3) &= \frac{1}{2}\left[\varphi(x_1, x_2, x_3) + \varphi(x_2, x_1, x_3)\right] \,, & \text{(D3)} \\ A_1(x_1, x_2, x_3) &= \frac{1}{2}\left[\varphi(x_2, x_1, x_3) - \varphi(x_1, x_2, x_3)\right] \,. & \text{(D4)} \end{aligned}$$

The asymptotic form - only the leading conformal spin contribution - of $\varphi(x_1, x_2, x_3, \mu)$ reads

$$\varphi_{Asy}(x_1, x_2, x_3, \mu) = 120 x_1 x_2 x_3 \phi_3^0(\mu), \quad (\phi_3^0 \equiv f_N) \,. \tag{D5}$$

Including next-to leading conformal spin one gets [2]

$$\varphi(x_1, x_2, x_3, \mu) = \varphi_{Asy}(x_1, x_2, x_3, \mu)\left[1 + \tilde{\phi}_3^-(\mu)(x_1 - x_2) + \tilde{\phi}_3^+(\mu)(1 - 3x_3)\right] \,, \tag{D6}$$

with

$$\tilde{\phi}_3^- = \frac{\phi_3^-}{\phi_3^0} \,, \qquad\qquad \tilde{\phi}_3^+ = \frac{\phi_3^+}{\phi_3^0} \,. \tag{D7}$$

In the literature also second moments of the leading-twist distribution amplitude were determined with QCD sum rules [29, 30, 37]. With this information one can build models for $\varphi(x_1, x_2, x_3)$ at a certain renormalization scale μ, including next-to-next-to leading conformal spin. We will use the model from [30] $\varphi^{COZ}(x_1, x_2, x_3)$ and the model from [37] $\varphi^{KS}(x_1, x_2, x_3)$:

$$\begin{aligned} \varphi^{COZ}(x_1, x_2, x_3) &= \varphi_{Asy}(x_1, x_2, x_3) \\ &\quad \left[23.814 x_1^2 + 12.978 x_2^2 + 6.174 x_3^2 + 5.88 x_3 - 7.098\right] \,, & \text{(D8)} \\ \varphi^{KS}(x_1, x_2, x_3) &= \varphi_{Asy}(x_1, x_2, x_3) \\ &\quad \left[20.16 x_1^2 + 15.12 x_2^2 + 22.68 x_3^2 - 6.72 x_3 + 1.68(x_1 - x_2) - 5.04\right] \,. & \text{(D9)} \end{aligned}$$

Bolz and Kroll derived a very simple model using some experimental constraints [47]. Their model for the leading-twist distribution amplitude reads

$$\varphi^{BK}(x_1, x_2, x_3) = \frac{1}{2}\varphi_{Asy}(x_1, x_2, x_3)(1 + 3x_1) \,. \tag{D10}$$

Based on the lattice calculations of φ^{100}, φ^{001}, φ^{101}, φ^{200} and φ^{002} in [3, 4] and Eq. (C1) we have obtained the model

$$\begin{aligned} \varphi^{LAT}(x_1, x_2, x_3) = \varphi_{Asy}(x_1, x_2, x_3)\big(&- 0.401 + 29.214 x_1 - 44.542 x_2 + 7.664 x_3 \\ &+ 12.561 x x_2 + 31.748 x_1 x_3 - 103.09 x_2 x_3 \\ &- 41.880 x_1^2 + 92.958 x_2^2 + 17.836 x_3^2\big) \,. \end{aligned} \tag{D11}$$

---

[1] V. L. Chernyak and A. R. Zhitnitsky, "Asymptotic Behavior of Exclusive Processes in QCD," *Phys. Rept.* **112** (1984) 173.

[2] V. Braun, R. J. Fries, N. Mahnke, and E. Stein, "Higher twist distribution amplitudes of the nucleon in QCD," *Nucl. Phys.* **B589** (2000) 381–409, `arXiv:hep-ph/0007279`.

[3] **QCDSF** Collaboration, M. Göckeler *et al.*, "Moments of nucleon distribution amplitudes from irreducible three-quark operators," *PoS* **LAT2007** (2007) 147, `arXiv:0710.2489 [hep-lat]`.

[4] M. Göckeler *et al.*, "Nucleon distribution amplitudes from lattice QCD," *Phys. Rev. Lett.* **101** (2008) 112002, `arXiv:0804.1877 [hep-lat]`.

[5] **QCDSF** Collaboration, V. M. Braun *et al.*, "Nucleon distribution amplitudes and proton decay matrix elements on the lattice," `arXiv:0811.2712 [hep-lat]`.

[6] V. M. Braun, A. Lenz, and M. Wittmann, "Nucleon form factors in QCD," *Phys. Rev.* **D73** (2006) 094019,`arXiv:hep-ph/0604050`.

[7] V. L. Chernyak and A. R. Zhitnitsky, "Asymptotic Behavior of Hadron Form-Factors in Quark Model. ," *JETP Lett.* **25** (1977) 510.

[8] V. L. Chernyak and A. R. Zhitnitsky, "Asymptotics of Hadronic Form-Factors in the Quantum Chromodynamics. ," *Sov. J. Nucl. Phys.* **31** (1980) 544–552.

[9] V. L. Chernyak, A. R. Zhitnitsky, and V. G. Serbo, "Asymptotic hadronic form-factors in quantum chromodynamics," *JETP Lett.* **26** (1977) 594–597.

[10] V. L. Chernyak, V. G. Serbo, and A. R. Zhitnitsky, "Calculation of asymptotics of the pion electromagnetic form-factor in the QCD perturbation theory.," *Sov. J. Nucl. Phys.* **31** (1980) 552–558.

[11] A. V. Radyushkin, "Deep elastic processes of composite particles in field theory and asymptotic freedom," `arXiv:hep-ph/0410276`.

[12] A. V. Efremov and A. V. Radyushkin, "Asymptotical Behavior of Pion Electromagnetic Form-Factor in QCD," *Theor. Math. Phys.* **42** (1980) 97–110.

[13] A. V. Efremov and A. V. Radyushkin, "Factorization and Asymptotical Behavior of Pion Form- Factor in QCD," *Phys. Lett.* **B94** (1980) 245–250.

[14] G. P. Lepage and S. J. Brodsky, "Exclusive Processes in Quantum Chromodynamics: Evolution Equations for Hadronic Wave Functions and the Form-Factors of Mesons," *Phys. Lett.* **B87** (1979) 359–365.

[15] G. P. Lepage and S. J. Brodsky, "Exclusive Processes in Perturbative Quantum Chromodynamics," *Phys. Rev.* **D22** (1980) 2157.

[16] V. M. Braun, A. Lenz, N. Mahnke, and E. Stein, "Light-cone sum rules for the nucleon form factors," *Phys. Rev.* **D65** (2002) 074011, `arXiv:hep-ph/0112085`.

[17] I. I. Balitsky, V. M. Braun, and A. V. Kolesnichenko, "Radiative Decay $\Sigma^+ \to p\gamma$ in Quantum Chromodynamics," *Nucl. Phys.* **B312** (1989) 509–550.

[18] V. L. Chernyak and I. R. Zhitnitsky, "B meson exclusive decays into baryons," *Nucl. Phys.* **B345** (1990) 137–172.

[19] **Jefferson Lab Hall A** Collaboration, M. K. Jones *et al.*, "G_{Ep}/G_{Mp} ratio by polarization transfer in $e + p \to e + p$," *Phys. Rev. Lett.* **84** (2000) 1398–1402, `arXiv:nucl-ex/9910005`.

[20] O. Gayou *et al.*, "Measurements of the elastic electromagnetic form factor ratio $\mu_p G_{Ep}/G_{Mp}$ via polarization transfer," *Phys. Rev.* **C64** (2001) 038202.

[21] **Jefferson Lab Hall A** Collaboration, O. Gayou *et al.*, "Measurement of G_{Ep}/G_{Mp} in $e+p \to e+p$ to $Q^2 = 5.6\,\text{GeV}^2$," *Phys. Rev. Lett.* **88** (2002) 092301, `arXiv:nucl-ex/0111010`.

[22] V. Punjabi *et al.*, "Proton elastic form factor ratios to $Q^2 = 3.5$ GeV^2 by polarization transfer," *Phys. Rev.* **C71** (2005) 055202, `arXiv:nucl-ex/0501018`.

[23] C. F. Perdrisat, V. Punjabi, and M. Vanderhaeghen, "Nucleon electromagnetic form factors," *Prog. Part. Nucl. Phys.* **59** (2007) 694–764, `arXiv:hep-ph/0612014`.

[24] V. M. Braun, A. Khodjamirian, and M. Maul, "Pion form factor in QCD at intermediate momentum transfers," *Phys. Rev.* **D61** (2000) 073004, `arXiv:hep-ph/9907495`.

[25] Y. Aoki, C. Dawson, J. Noaki, and A. Soni, "Proton decay matrix elements with domain-wall fermions," *Phys. Rev.* **D75** (2007) 014507, `arXiv:hep-lat/0607002`.

[26] Y. Aoki *et al.*, "Proton lifetime bounds from chirally symmetric lattice QCD," `arXiv:0806.1031 [hep-lat]`.

[27] M.-q. Huang and D.-W. Wang, "Light-cone QCD sum rules for the semileptonic decay $\Lambda_b \to pl\bar{\nu}$," *Phys. Rev.* **D69** (2004) 094003, `arXiv:hep-ph/0401094`.

[28] A. J. Lenz, "Form factors of baryons within the framework of light-cone sum rules," *AIP Conf. Proc.* **964** (2007) 77–83, `arXiv:0708.0633 [hep-ph]`.

[29] V. L. Chernyak and I. R. Zhitnitsky, "Nucleon Wave Function and Nucleon Form-Factors in QCD," *Nucl. Phys.* **B246** (1984) 52–74.

[30] V. L. Chernyak, A. A. Ogloblin, and I. R. Zhitnitsky, "The wave functions of the octet baryons," *Z. Phys.* **C42** (1989) 569.

[31] M. A. Shifman, A. I. Vainshtein, and V. I. Zakharov, "QCD and Resonance Physics. Sum Rules," *Nucl. Phys.* **B147** (1979) 385–447.

[32] V. M. Braun and A. Lenz, "On the SU(3) symmetry-breaking corrections to meson distribution amplitudes," *Phys. Rev.* **D70** (2004) 074020, `arXiv:hep-ph/0407282`.

[33] P. Ball, V. M. Braun, and A. Lenz, "Higher-twist distribution amplitudes of the K meson in QCD," *JHEP* **05** (2006) 004, `arXiv:hep-ph/0603063`.

[34] P. Ball, V. M. Braun, and A. Lenz, "Twist-4 Distribution Amplitudes of the K* and ϕ Mesons in QCD," *JHEP* **08** (2007) 090, `arXiv:0707.1201 [hep-ph]`.

[35] V. M. Braun *et al.*, "Moments of pseudoscalar meson distribution amplitudes from the lattice," *Phys. Rev.* **D74** (2006) 074501, `arXiv:hep-lat/0606012`.

[36] **UKQCD** Collaboration, P. A. Boyle *et al.*, “A lattice computation of the first moment of the kaon’s distribution amplitude,” *Phys. Lett.* **B641** (2006) 67–74, `arXiv:hep-lat/0607018`.

[37] I. D. King and C. T. Sachrajda, “Nucleon Wave Functions and QCD Sum Rules,” *Nucl. Phys.* **B279** (1987) 785.

[38] B. L. Ioffe, “Calculation of Baryon Masses in Quantum Chromodynamics,” *Nucl. Phys.* **B188** (1981) 317–341.

[39] Y. Chung, H. G. Dosch, M. Kremer, and D. Schall, “Baryon Sum Rules and Chiral Symmetry Breaking,” *Nucl. Phys.* **B197** (1982) 55.

[40] V. M. Belyaev and B. L. Ioffe, “Determination of Baryon and Baryonic Resonance Masses from QCD Sum Rules. 1. Nonstrange Baryons,” *Sov. Phys. JETP* **56** (1982) 493–501.

[41] D. B. Leinweber, “QCD Sum Rule Analysis of Spin Orbit Splitting in Baryons,” *Ann. Phys.* **198** (1990) 203.

[42] B. L. Ioffe, “QCD at low energies,” *Prog. Part. Nucl. Phys.* **56** (2006) 232–277, `arXiv:hep-ph/0502148`.

[43] M. Jamin, “Radiative corrections for baryonic correlators,” *Z. Phys.* **C37** (1988) 635.

[44] A. Lenz, M. Wittmann, and E. Stein, “Improved light-cone sum rules for the electromagnetic form factors of the nucleon,” *Phys. Lett.* **B581** (2004) 199–206, `arXiv:hep-ph/0311082`.

[45] G. Martinelli and C. T. Sachrajda, “The quark distribution amplitude of the proton: A lattice computation of the lowest two moments,” *Phys. Lett.* **B217** (1989) 319.

[46] T. Kaltenbrunner, M. Göckeler, and A. Schäfer, “Irreducible Multiplets of Three-Quark Operators on the Lattice: Controlling Mixing under Renormalization,” *Eur. Phys. J.* **C55** (2008) 387–401, `arXiv:0801.3932 [hep-lat]`.

[47] J. Bolz and P. Kroll, “Modelling the nucleon wave function from soft and hard processes,” *Z. Phys.* **A356** (1996) 327, `arXiv:hep-ph/9603289`.

[48] Z.-G. Wang, S.-L. Wan, and W.-M. Yang, “Scalar form-factor of the proton with light-cone QCD sum rules,” *Phys. Rev.* **D73** (2006) 094011, `arXiv:hep-ph/0601025`.

[49] Z.-G. Wang, S.-L. Wan, and W.-M. Yang, “Axial form-factor and induced pseudoscalar form-factor of the nucleons,” *Eur. Phys. J.* **C47** (2006) 375–384, `arXiv:hep-ph/0601060`.

[50] T. M. Aliev and M. Savci, “Scalar form factor of the nucleon and nucleon - scalar meson coupling constant in QCD,” *Phys. Rev.* **D75** (2007) 045006, `arXiv:hep-ph/0612144`.

[51] T. M. Aliev and M. Savci, “Nucleon form factors induced by isovector and isoscalar axial-vector currents in QCD,” *Phys. Lett.* **B656** (2007) 56–66, `arXiv:0711.1757 [hep-ph]`.

[52] T. M. Aliev, K. Azizi, A. Ozpineci, and M. Savci, “Nucleon Electromagnetic Form Factors in QCD,” *Phys. Rev.* **D77** (2008) 114014, `arXiv:0802.3008 [hep-ph]`.

[53] V. M. Braun, A. Lenz, G. Peters, and A. V. Radyushkin, “Light cone sum rules for $\gamma^* N \to \Delta$ transition form factors,” *Phys. Rev.* **D73** (2006) 034020, `arXiv:hep-ph/0510237`.

[54] J. Rohrwild, “Light-cone sum rules for the $N\gamma\Delta$ transitions for real photons,” *Phys. Rev.* **D75** (2007) 074025, `arXiv:hep-ph/0701085`.

[55] T. M. Aliev, K. Azizi, and A. Ozpineci, “Light Cone QCD Sum Rules Analysis of the Axial $N \to \Delta$ Transition Form Factors,” *Nucl. Phys.* **A799** (2008) 105–126, `arXiv:0707.1592 [hep-ph]`.

[56] V. M. Braun *et al.*, “Electroproduction of the N*(1535) resonance at large momentum transfer,” `arXiv:0902.3087 [hep-ph]`.

[57] V. M. Braun, D. Y. Ivanov, A. Lenz, and A. Peters, “Deep inelastic pion electroproduction at threshold,” *Phys. Rev.* **D75** (2007) 014021, `arXiv:hep-ph/0611386`.

[58] V. M. Braun, D. Y. Ivanov, and A. Peters, “Threshold Pion Electroproduction at Large Momentum Transfers,” *Phys. Rev.* **D77** (2008) 034016, `arXiv:0710.3265 [hep-ph]`.

[59] V. M. Braun, D. Y. Ivanov, A. Lenz, and A. Peters, “Threshold Pion Production at Large Momentum Transfers,” `arXiv:0901.3184 [hep-ph]`.

[60] M.-Q. Huang and D.-W. Wang, “Semileptonic decay $\Lambda_c \to \Lambda l^+ \nu$ from QCD light-cone sum rules,” `arXiv:hep-ph/0608170`.

[61] Z. G. Wang, “Analysis of the Sigma n form factors with light-cone QCD sum rules,” *J. Phys.*​**G34** (2007) 493–504, `arXiv:hep-ph/0609155`.

[62] Y.-m. Wang, Y. Li, and C.-D. Lu, “Rare Decays of $\Lambda_b \to \Lambda + \gamma$ and $\Lambda_b \to \Lambda + l^+ l^-$ in the Light-cone Sum Rules,” `arXiv:0804.0648 [hep-ph]`.

[63] Y.-L. Liu and M.-Q. Huang, “Distribution amplitudes of Σ and Λ and their electromagnetic form factors,” `arXiv:0811.1812 [hep-ph]`.

[64] Y.-L. Liu, M.-Q. Huang, and D.-W. Wang, “Light-cone QCD Sum Rules for Λ Baryon Electromagnetic Form Factors and its magnetic moment,” `arXiv:0810.4973 [hep-ph]`.

[65] K. Passek-Kumericki and G. Peters, “Nucleon Form Factors to Next-to-Leading Order with Light- Cone Sum Rules,” *Phys. Rev.* **D78** (2008) 033009, `arXiv:0805.1758 [hep-ph]`.

[66] L. Andivahis *et al.*, “Measurements of the electric and magnetic form-factors of the proton from $\mathrm{Q}^2 = 1.75$ $(\mathrm{GeV/c})^2$ to 8.83 $(\mathrm{GeV/c})^2$,” *Phys. Rev.* **D50** (1994) 5491–5517.

[67] R. C. Walker *et al.*, “Measurements of the proton elastic form-factors for 1- $(\mathrm{GeV/c})^2 \leq Q^2 \leq 3(\mathrm{GeV/c})^2$ at SLAC,” *Phys. Rev.* **D49** (1994) 5671–5689.

[68] J. Litt *et al.*, “Measurement of the ratio of the proton form factors, G(E) / G(M), at high momentum transfer and the question of sacling,” *Phys. Lett.* **B31** (1970) 40–44.

[69] C. Berger, V. Burkert, G. Knop, B. Langenbeck, and K. Rith, “Electromagnetic form-factors of the proton at squared four momentum transfers between 10 fm^{-2} and 50 fm^{-2},” *Phys. Lett.* **B35** (1971) 87.

[70] T. Janssens, R. Hofstadter, E. B. Hughes, and M. R. Yearian, “Proton form factors from elastic electron-proton scattering,” *Phys. Rev.* **142** (1966) 922–931.

[71] **E94110** Collaboration, M. E. Christy *et al.*, “Measurements of electron proton elastic cross sections for 0.4 $(\mathrm{GeV/c})^2 < Q^2 <$5.5 $(\mathrm{GeV/c})^2$,” *Phys. Rev.* **C70** (2004) 015206, `arXiv:nucl-ex/0401030`.

[72] I. A. Qattan *et al.*, “Precision Rosenbluth measurement of the proton elastic form factors,” *Phys. Rev. Lett.* **94** (2005) 142301, `arXiv:nucl-ex/0410010`.

[73] W. Bartel *et al.*, “Measurement of proton and neutron electromagnetic form- factors at squared four momentum transfers up to 3 $(\mathrm{GeV/c})^2$,” *Nucl. Phys.* **B58** (1973) 429–475.

[74] L. E. Price *et al.*, “Backward-angle electron-proton elastic scattering and proton electromagnetic form-factors,” *Phys. Rev.* **D4** (1971) 45–53.

[75] J. Arrington, “How well do we know the electromagnetic form factors of the proton?,” *Phys. Rev.* **C68** (2003) 034325, `arXiv:nucl-ex/0305009`.

[76] C. B. Crawford *et al.*, “Measurement of the proton electric to magnetic form factor ratio from H-1(pol.)(e(pol.),e’ p),” *Phys. Rev. Lett.* **98** (2007) 052301, `arXiv:nucl-ex/0609007`.

[77] **Bates FPP** Collaboration, B. D. Milbrath *et al.*, “A comparison of polarization observables in electron scattering from the proton and deuteron,” *Phys. Rev. Lett.* **80** (1998) 452–455, `arXiv:nucl-ex/9712006`.

[78] **A1** Collaboration, T. Pospischil *et al.*, “Measurement of G(E(p))/G(M(p)) via polarization transfer at $\mathrm{Q}^2 = 0.4$ $(\mathrm{GeV/c})^2$,” *Eur. Phys. J.* **A12** (2001) 125–127.

[79] M. Jones *private communication* .

[80] A. Lung *et al.*, “Measurements of the electric and magnetic form-factors of the neutron from $\mathrm{Q}^2 = 1.75$ $(\mathrm{GeV/c})^2$ to 4 $(\mathrm{GeV/c})^2$,” *Phys. Rev. Lett.* **70** (1993) 718–721.

[81] G. Kubon *et al.*, “Precise neutron magnetic form factors,” *Phys. Lett.* **B524** (2002) 26–32, `arXiv:nucl-ex/0107016`.

[82] H. Anklin *et al.*, “Precise measurements of the neutron magnetic form factor,” *Phys. Lett.* **B428** (1998) 248–253.

[83] **E93-038** Collaboration, R. Madey *et al.*, “Measurements of G(E)(n)/G(M)(n) from the H-2(e(pol.),e’ n(pol.))H-1 reaction to $\mathrm{Q}^2 = 1.45$ $(\mathrm{GeV/c})^2$,” *Phys. Rev. Lett.* **91** (2003) 122002, `arXiv:nucl-ex/0308007`.

[84] W. Xu *et al.*, “The transverse asymmetry A(T’) from quasielastic polarized He-3(pol.)(e(pol.),e’) process and the neutron magnetic form factor,” *Phys. Rev. Lett.* **85** (2000) 2900–2904, `arXiv:nucl-ex/0008003`.

[85] **Jefferson Lab E95-001** Collaboration, W. Xu *et al.*, “PWIA extraction of the neutron magnetic form factor from quasi-elastic He-3(pol.)(e(pol.),e’) at $\mathrm{Q}^2 = 0.3$ $(\mathrm{GeV/c})^2$ to 0.6 $(\mathrm{GeV/c})^2$,” *Phys. Rev.* **C67** (2003) 012201, `arXiv:nucl-ex/0208007`.

[86] H. Anklin *et al.*, “Precision measurement of the neutron magnetic form- factor,” *Phys. Lett.* **B336** (1994) 313–318.

[87] **E93026** Collaboration, H. Zhu *et al.*, “A measurement of the electric form-factor of the neutron through d(pol.)(e(pol.),e’ n)p at $\mathrm{Q}^2 = 0.5$ $(\mathrm{GeV/c})^2$,” *Phys. Rev. Lett.* **87** (2001) 081801, `arXiv:nucl-ex/0105001`.

[88] D. Rohe *et al.*, “Measurement of the neutron electric form factor G(en) at 0.67 $(\mathrm{GeV/c})^2$ via He-3(pol.)(e(pol.),e’ n),” *Phys. Rev. Lett.* **83** (1999) 4257–4260.

[89] C. Herberg *et al.*, “Determination of the neutron electric form factor in the D(e,e’ n)p reaction and the influence of nuclear binding,” *Eur. Phys. J.* **A5** (1999) 131–135.

[90] M. Ostrick *et al.*, “Measurement of the neutron electric form factor G(E,n) in the quasifree H-2(e(pol.),e’ n(pol.))p reaction,” *Phys. Rev. Lett.* **83** (1999) 276–279.

[91] J. Becker *et al.*, “Determination of the neutron electric form factor from the reaction He-3(e,e’ n) at medium momentum transfer,” *Eur. Phys. J.* **A6** (1999) 329–344.

[92] T. Eden *et al.*, “Electric form-factor of the neutron from the H-2 (e (polarized), e-prime n (polarized)) H-1 reaction at $\mathrm{Q}^2 = 0.255$ $(\mathrm{GeV/c})^2$,” *Phys. Rev.* **C50** (1994) 1749–1753.

[93] **Jefferson Laboratory E93-038** Collaboration, B. Plaster *et al.*, “Measurements of the neutron electric to magnetic form factor ratio G(E(n))/G(M(n)) via the H-2(e(pol.),e’ n(pol.))H-1 reaction to $\mathrm{Q}^2 = 1.45$ $(\mathrm{GeV/c})^2$,” *Phys. Rev.* **C73** (2006) 025205, `arXiv:nucl-ex/0511025`.

[94] **BLAST** Collaboration, E. Geis *et al.*, “The Charge Form Factor of the Neutron at Low Momentum Transfer from the ${}^2\vec{\mathrm{H}}(\vec{\mathrm{e}},\mathrm{e}'\mathrm{n})\mathrm{p}$ Reaction,” `arXiv:0803.3827 [nucl-ex]`.

[95] D. I. Glazier *et al.*, “Measurement of the Electric Form Factor of the Neutron at $Q^2 = 0.3 - 0.8(GeV/c)^2$,” *Eur. Phys. J.* **A24** (2005) 101–109, `arXiv:nucl-ex/0410026`.

[96] **Jefferson Lab E93-026** Collaboration, G. Warren *et al.*, “Measurement of the electric form factor of the neutron at $\mathrm{Q}^2 = 0.5$ $(\mathrm{GeV/c})^2$ and 1.0 $(\mathrm{GeV/c})^2$,” *Phys. Rev. Lett.* **92** (2004) 042301, `arXiv:nucl-ex/0308021`.

[97] J. Bermuth *et al.*, “The neutron charge form factor and target analyzing powers from He-3(pol.)(e(pol.),e’ n) scattering,” *Phys. Lett.* **B564** (2003) 199–204, `arXiv:nucl-ex/0303015`.

[98] I. Passchier *et al.*, “The charge form factor of the neutron from the reaction H-2(pol.)(e(pol.),e’ n)p,” *Phys. Rev. Lett.* **82** (1999) 4988–4991, `arXiv:nucl-ex/9907012`.

[99] J. Golak, G. Ziemer, H. Kamada, H. Witala, and W. Gloeckle, “Extraction of electromagnetic neutron form factors through inclusive and exclusive polarized electron scattering on polarized He-3 target,” *Phys. Rev.* **C63** (2001) 034006, `arXiv:nucl-th/0008008`.

[100] R. Schiavilla and I. Sick, “Neutron charge form factor at large q^2,” *Phys. Rev.* **C64** (2001) 041002, `arXiv:nucl-ex/0107004`.

[101] S. Galster *et al.*, “Elastic electron - deuteron scattering and the electric neutron form-factor at four momentum transfers $5\ \mathrm{fm}^{-2} < q^2 < 14\ \mathrm{fm}^{-2}$,” *Nucl. Phys.* **B32** (1971) 221–237.

[102] J. J. Kelly, “Simple parametrization of nucleon form factors,” *Phys. Rev.* **C70** (2004) 068202.

[103] A. Bodek, S. Avvakumov, R. Bradford, and H. Budd, “Vector and Axial Nucleon Form Factors:A Duality Constrained

Parameterization," *Eur. Phys. J.* **C53** (2008) 349–354, `arXiv:0708.1946 [hep-ex]`.
[104] P. Stoler, "Baryon form-factors at high Q^2 and the transition to perturbative QCD," *Phys. Rept.* **226** (1993) 103–171.
[105] L. M. Stuart *et al.*, "Measurements of the Delta(1232) transition form factor and the ratio sigma(n)/sigma(p) from inelastic electron proton and electron deuteron scattering," *Phys. Rev.* **D58** (1998) 032003, `arXiv:hep-ph/9612416`.
[106] W. Bartel *et al.*, "Electroproduction of pions near the Delta(1236) isobar and the form-factor of G*(M)(q^2) of the (gamma N Delta) vertex," *Phys. Lett.* **B28** (1968) 148–151.
[107] S. Stein *et al.*, "Electron Scattering at 4-Degrees with Energies of 4.5-GeV - 20-GeV," *Phys. Rev.* **D12** (1975) 1884.
[108] F. Foster and G. Hughes, "Electroproduction of nucleon resonances," *Rept. Prog. Phys.* **46** (1983) 1445–1489.
[109] S. S. Kamalov, S. N. Yang, D. Drechsel, O. Hanstein, and L. Tiator, "$\gamma * N - - > \Delta$ transition form factors: A new analysis of the JLab data on p(e,e' p)pi0 at $Q^2 = 2.8$ (GeV/c)^2 and 4.0 (GeV/c)^2," *Phys. Rev.* **C64** (2001) 032201, `arXiv:nucl-th/0006068`.
[110] J. C. Alder *et al.*, "Pi0 electroproduction at the first resonance at momentum transfers Q^2=0.6, 1.0 and 1.56 GeV^2," *Nucl. Phys.* **B46** (1972) 573–592.
[111] V. V. Frolov *et al.*, "Electroproduction of the Delta(1232) resonance at high momentum transfer," *Phys. Rev. Lett.* **82** (1999) 45–48, `arXiv:hep-ex/9808024`.
[112] **CLAS** Collaboration, K. Joo *et al.*, "Q^2 dependence of quadrupole strength in the gamma* p → Delta(1232)+ → p pi0 transition," *Phys. Rev. Lett.* **88** (2002) 122001, `arXiv:hep-ex/0110007`.
[113] V. M. Braun, A. N. Manashov, and J. Rohrwild, "Baryon Operators of Higher Twist in QCD and Nucleon Distribution Amplitudes," `arXiv:0806.2531 [hep-ph]`.
[114] M. Bergmann and N. G. Stefanis, "Evolution effects on the nucleon distribution amplitude," `arXiv:hep-ph/9403210`.
[115] M. Bergmann, W. Schroers, and N. G. Stefanis, "Large-order trend of the anomalous-dimensions spectrum of trilinear twist-3 quark operators," *Phys. Lett.* **B458** (1999) 109–116, `arXiv:hep-ph/9903339`.
[116] V. M. Braun, S. E. Derkachov, G. P. Korchemsky, and A. N. Manashov, "Baryon distribution amplitudes in QCD," *Nucl. Phys.* **B553** (1999) 355–426, `arXiv:hep-ph/9902375`.
[117] To be precise, we have determined ϕ^{002}, ϕ^{101} and ϕ^{110} from the BLW description and ϕ^{200}, ϕ^{020} and ϕ^{011} from momentum conservation.